A covariance based framework for the propagation of correlated uncertainty in frequency based dynamic sub-structuring

J.W.R. Meggitt[1], A.T. Moorhouse[1]

[1]*Acoustics Research Centre, University of Salford, Greater Manchester, M5 4WT*

Abstract

Dynamic sub-structuring (DS) is the procedure by which the passive properties (i.e. frequency response functions) of an assembled structure are predicted from those of its constituent sub-structures. In this paper we are concerned with the propagation of *correlated* uncertainty through such a prediction. In this work a first-order covariance based propagation framework is derived based on the primal and dual formulations of the sub-structuring problem and the complex bivariate description of FRF uncertainty. The proposed framework is valid also in the case of sub-structure decoupling, since the underlying equations are of an identical form. The present paper extends previous work into a more general framework by accounting for the presence of correlated uncertainty. This is important as recent work has demonstrated that the neglect inter-FRF correlation (i.e. the correlated uncertainty associated with impact-based FRF measurements) can lead to large errors in uncertainty estimates. Efficient algorithms are introduced for implementation of the proposed framework. Results are compared against Monte-Carlo simulations and shown to be in good agreement for both correlated, uncorrelated and mixed uncertainty. These results further illustrate that the neglect of inter-FRF correlation, when physically present, can lead to large over-estimations in the uncertainty of coupled structures. This result justifies use of the proposed framework.

Keywords: Uncertainty propagation, dynamic sub-structuring, operator uncertainty, frequency response functions, structural dynamics

1. Introduction

Dynamic sub-structuring (DS) is the procedure by which the passive properties (i.e. frequency response functions) of an assembled structure are predicted from those of its constituent sub-structures [1].[1]

Dynamic sub-structuring procedures are routinely employed to predict and/or analyse the dynamics of complex built-up structures, for example, in aerospace and automotive applications. Often, these structures are designed so as to conform to strict limits, be it to avoid structural fatigue and failure, or to promote passenger comfort. If such limits are to be met with confidence it is essential that reliable estimates of uncertainty are available. To this end, we are concerned with the propagation of uncertainty through DS procedures.

As a topic of research, DS has received considerable attention over the past 5 decades, a comprehensive review of which may be found in [1]. Similarly, the field of structural dynamic uncertainty is vast (see [2, 3, 4] for notable review papers and special issues). The intersection of these two fields however, the study of uncertainty in DS, is comparatively sparse.

The propagation of uncertainty in the context of DS was previously considered in [5] under the assumption of uncorrelated sub-structure uncertainty. In [6] the same authors use a similar approach to investigate the propagation of uncertainty in the context of substructure decoupling. Although effective in estimating the uncertainty in coupled (or uncoupled) FRFs based on the presence of additive noise, in practice there exists an additional source of uncertainty due to human error in the measurement procedure, referred to here as operator uncertainty. It was shown by Meggitt [7] that if the excitation position of a measured frequency response function (FRF) is considered as a random variable

[1]More recently, DS procedures have been used also to *decouple* structures, thus obtaining their free interface dynamics.

(i.e. to model the inaccuracy in excitation position when performing impact-based FRF measurements), then there exists a correlation between FRFs of shared excitation (i.e. within each column of an FRF matrix). It was further shown that this inter-FRF correlation influences greatly the propagation of uncertainty through a matrix inversion. This is of particular relevance to DS where matrix inversions are an essential step. It is the influence of operator uncertainty, or correlated uncertainty in general, in the context of DS that motivates this work.

Note that, although operator uncertainty is the most likely origin, inter-FRF correlations are also introduced when the notion of ensemble uncertainty is considered. For an ensemble of nominally identical sub-structures, for example those coming off a production line, the uncertainty present due to manufacturing tolerances will likely generate inter-FRF correlations, since the underlying uncertainty is shared among all degrees of freedom (DoFs). For example, uncertainty in the distribution of mass across nominally identical plate-like structures will introduce a correlation between any two FRFs as they are governed by the same underlying uncertainty through the dynamics of the structure. The proposed framework remains valid in this context as it does not depend upon the source of correlation, only that it may be described through an appropriate covariance matrix.

Acknowledging the notion of ensemble uncertainty, Kammer and Krattiger [8] considered the propagation of sub-structure uncertainty onto an assembled structure for the purpose of test-analysis correlation metrics (i.e. some comparison between experimental and numerical predictions [9]). The authors adopted a complex description of uncertainty, utilising the complex covariance and relation matrices (in the present paper an alternate bivariate description of complex uncertainty is used). Whilst sub-structure uncertainty is defined generally, such that any inter-FRF correlations are accounted for, the propagation is formulated in the modal domain using a Craig Bampton Component Mode Synthesis approach. As such, its application to directly measured FRFs is not straightforward.

In the present paper we consider sub-structure uncertainty directly in terms of their measured (or modelled) FRFs. The proposed framework complements recent work by Meggitt et al. [10], where a framework was established for estimating the uncertainty of inversely determined blocked forces. Blocked forces are often used to prescribe the operational loading of an active sub-structure, for example a vibration source, such that the operational response of an assembled structure can be predicted [11], for example, in the construction of a Virtual Acoustic Prototype (VAP) [12]. The framework proposed herein, alongside that of [10], would provide the necessary tools to accurately estimate the uncertainty in an operational response prediction of a complex built-up structure.

The experimental uncertainty associated with measured FRFs may be categorised as either measurement or operator based [10]. Measurement uncertainty is typically of an aleatory nature and describes the cumulative effect of noise sources in the measurement signal path and computational post processing, for example, external disturbances, thermo-electrical noise, sampling error, finite precision, etc. Measurement uncertainty is typically considered to be of an uncorrelated nature. Operator uncertainty may be regarded epistemic and describes the effect of human error in the measurement procedure, for example, inconsistent location and/or orientation of applied forces during the measurement of FRFs. In [7] it was shown that operator uncertainty is of a correlated nature. An appropriate framework must be capable of propagating uncertainty of both forms.

Further to the experimental uncertainty associated with measured FRFs, DS procedures are subject to 'model uncertainty'. Model uncertainties are those that arise when an approximate model is used to describe the physical problem, for example, assuming sub-structure linearity and/or time invariance which is not realised in practice [10]. The most likely origin of model uncertainty, in the context of DS, is the neglect (or misplacement) of important DoFs when characterising a sub-structure's interface dynamics. Incomplete interface descriptions are often encountered in practice due to the experimental challenges associated with measuring rotational and in-plane DoFs. Recent works, however, have begun to acknowledge this difficulty and propose techniques that avoid the need to apply/measure troublesome excitations/responses [13, 14, 15, 16, 17]. Although a potentially significant factor, the influence of model uncertainty, and its propagation, in the context of DS, is considered beyond the scope of this work. The present paper will focus instead on the propagation of *experimental* FRF uncertainty.

The presence of measurement uncertainty in measured FRFs is often modelled in the form,

$$\mathbf{Y}^{\mathbf{meas}} = \mathbf{Y} + \epsilon \tag{1}$$

where $\mathbf{Y}$ represents the underlying true FRF and ϵ an additive noise that describes the associated measurement uncertainty. It is typically assumed that ϵ has zero mean. The nature of its correlation varies among the literature. In general, it is assumed that elements of ϵ are uncorrelated with one another, but that there may exist a correlation

between the real and imaginary components of a given element. In [18, 19] it was assumed that the real and imaginary components were uncorrelated and shared the same variance. In [20, 5] real and imaginary components where assumed uncorrelated, but of different variance. Others have treated the uncertainty more generally by allowing not only a different variance for real and imaginary components, but a covariance between them [21, 22].

In [7] it was shown that an additional form of uncertainty is present due to variability in the excitation position of measured FRFs. Referred to as operator uncertainty, conceptually it may be modelled in the form,

$$\mathbf{Y}^{\mathbf{meas}} = \mathbf{Y}(a_0 + \mathbf{a}) \tag{2}$$

where $\mathbf{Y}()$ represents an FRF function whose argument $a_0 + \mathbf{a}$ represents the excitation position. In this description, a_0 corresponds to the intended excitation position and $\mathbf{a}$ the random deviation about this position due to human error. Such an uncertainty leads to a correlation between elements of the FRF matrix that share an excitation (i.e. within a column) the magnitude of which is dependent upon the dynamics of the structure and the accuracy of the experimenter. Whilst the presence of such correlated uncertainty has been acknowledged in previous work [5], its influence on the estimation of uncertainty was not considered.

It is the aim of this paper to provide a general uncertainty propagation framework that encompasses both measurement (uncorrelated) and operator (correlated) based uncertainty,

$$\mathbf{Y}^{\mathbf{meas}} = \mathbf{Y}(a_0 + \mathbf{a}) + \epsilon. \tag{3}$$

This will be achieved by considering both the primal and dual formulations of the DS problem and applying a complex bivariate form of the law of error propagation (a first order covariance based propagation). This will lead to a set of equations that relate the uncertainty present in the uncoupled sub-structure FRF matrices to that of the coupled FRF matrix.

The remainder of this paper will be organised as follows. Section 2 will begin by introducing the bivariate description of complex uncertainty adopted in this work. Section 3 will go on to re-introduce the primal DS procedure for coupling structural elements. Following this, section 4 will focus on the derivation of appropriate uncertainty propagation formulae, before the problem of efficient numerical implementation is addressed in section 5. Section 6 will then demonstrate the proposed framework as part of a numerical study. Finally, section 7 will summarize the main findings of this work and draw some concluding remarks.

2. Treatment of Complex Uncertainty

The FRFs typically encountered in experimental structural dynamics are complex quantities, acquired through the ratio of Fourier transformed input and output signals [23]. Typical examples include accelerance, mobility and receptance, which are given as the ratio of acceleration, velocity and displacement, respectively, to an applied force [24].

Assuming a two parameter elliptical distribution (e.g. Gaussian), the statistical properties of a complex random variable (RV), $H \in \mathbb{C}$, such as an FRF, may be described generally using the bivariate variance-covariance matrix[2] [25, 26, 21, 22, 19] ,

$$\mathbf{\Sigma}_H = \begin{bmatrix} \sigma_{\Re(H)\Re(H)} & \sigma_{\Re(H)\Im(H)} \\ \sigma_{\Im(H)\Re(H)} & \sigma_{\Im(H)\Im(H)} \end{bmatrix} \tag{4}$$

where, $\sigma_{\Re(H)\Re(H)}$ is the variance of the real part of H, $\sigma_{\Im(H)\Im(H)}$ is the variance of the imaginary part of H, and $\sigma_{\Im(H)\Re(H)} = \sigma_{\Re(H)\Im(H)}$ is the covariance between them. Given two random variables, A and B, their covariance (or variance in the case that $A = B$) is given by,

$$\sigma_{AB} = \frac{1}{P} \sum_{i}^{P} \left(A_i - \mathbb{E}[A]\right) \left(B_i - \mathbb{E}[B]\right) \tag{5}$$

[2] hereafter we will use the term covariance matrix generally to describe both covariance and variance-covariance matrices

where, subscript i indicates the ith measurement of said variable, P is the total number of measurements taken, and $\mathbb{E}[]$ is the expectation operator. Equation 4 may readily be extended to describe the covariance *between* complex RVs,

$$\mathbf{\Sigma}_{H_1H_2} = \begin{bmatrix} \sigma_{\Re(H_1)\Re(H_2)} & \sigma_{\Re(H_1)\Im(H_2)} \\ \sigma_{\Im(H_1)\Re(H_2)} & \sigma_{\Im(H_1)\Im(H_2)} \end{bmatrix}. \tag{6}$$

Consequently, the uncertainty of a measured FRF matrix, $\mathbf{H} \in \mathbb{C}^{N\times M}$, is completely described, assuming that its elements follow a multivariate normal distribution, by the bivariate covariance matrix $\mathbf{\Sigma_H} \in \mathbb{R}^{2NM\times 2NM}$. Results supporting this assumption have been published in [7], where the correlated bivariate nature of impact based FRFs was shown experimentally.

To estimate $\mathbf{\Sigma_H}$, each measurement DoF must be excited repeatedly such that a series of P measurements are made. The user must then decide at what point in the preceding analysis to estimate the statistical properties of the data. As an example, one may consider the complex Fourier spectra of the input and output signals as the initial RVs and determine their associated covariance matrices. To acquire the covariance matrix of an FRF the Fourier spectra uncertainty must be propagated through the H1 (or H2) estimator function. Alternatively, one may consider the FRF itself as the RV and determine the bivariate FRF covariance matrix directly, thus avoiding the need to perform additional uncertainty propagations (the authors find this approach the most practical). This may be beneficial as each propagation stage incurs an additional uncertainty on the basis that linearity of the propagation function is assumed (see Appendix A). In this work it will be assumed that an appropriate FRF covariance matrix has been determined by whatever means (see for example Appendix A of [7]).

When dealing with the uncertainty of complex quantities it is important to note that these are typically represented in terms of their magnitude and phase, as opposed to their real and imaginary components. As such, it would be beneficial to provide some measure of the total variability in the complex quantity. Two common measures are the total dispersion (sum of variances) and the generalised variance (determinant of covariance matrix) [27]. Alternatively, the law of error propagation may be used to relate the uncertainty of an absolute value to that of the real and imaginary components,

$$\sigma^2_{|H|} = \begin{pmatrix} \frac{\Re(H)}{\sqrt{\Re(H)^2+\Im(H)^2}} & \frac{\Im(H)}{\sqrt{\Re(H)^2+\Im(H)^2}} \end{pmatrix} \begin{bmatrix} \sigma_{\Re(H)\Re(H)} & \sigma_{\Re(H)\Im(H)} \\ \sigma_{\Im(H)\Re(H)} & \sigma_{\Im(H)\Im(H)} \end{bmatrix} \begin{pmatrix} \frac{\Re(H)}{\sqrt{\Re(H)^2+\Im(H)^2}} \\ \frac{\Im(H)}{\sqrt{\Re(H)^2+\Im(H)^2}} \end{pmatrix}. \tag{7}$$

A similar procedure may be used to determine the uncertainty in phase angle, $\angle H = \tan^{-1}\left(\frac{\Im(H)}{\Re(H)}\right)$, although care must be taken so as to ensure the correct quadrant of the complex plane is considered. The above procedure would be necessary if, for example, uncertainty bounds were required on the absolute value (and/or phase) of a measured FRF.

Whilst the above provides a general description of complex uncertainty, the FRF literature has often assumed that $\mathbf{\Sigma}_H = \text{diag}(\sigma_{\Re(H)\Re(H)}, \sigma_{\Im(H)\Im(H)})$ and that $\mathbf{\Sigma}_{H_1H_2} = \mathbf{0}$, that is, the uncertainties are uncorrelated. It was shown in [7], however, that this assumption is invalid in the presence of operator uncertainty and can lead to large errors when propagating uncertainty through matrix inversions. A general treatment of complex uncertainty must therefore acknowledge the potential correlation *between* FRFs.

3. Dynamic Sub-structuring - Primal Formulation

Before considering the propagation of uncertainty, we will briefly reintroduce some general DS theory.

The mathematical coupling of structural elements can be performed in a variety of ways (i.e. using primal, dual or hybrid formulations). Although differing in their implementation, the underlying physics are the same. In any case, one must satisfy two conditions between all pairs of coupling DoFs; compatibility and equilibrium. Compatibility states that the relative motion (i.e. displacement, velocity, acceleration) between any two coupling DoFs is 0, i.e. $v_1 = v_2$, where v_1 and v_2 are the collocated boundary velocities of sub-structure 1 and 2, respectively. Equilibrium further states that the forces applied to pairs of coupling DoFs are equal and opposite, i.e. $g_1 = -g_2$.

In section 4 we will focus on the primal formulation of the DS problem (for its mathematical simplicity) and derive an uncertainty propagation framework (a dual formulation of the propagation framework is also provided in section 4.2). For completeness, we will reintroduce the primal formulation below. For an account of the dual formulation the reader is referred to [1].

The equations of motion for *P uncoupled* sub-structures may be expressed in a block diagonalised form as,

$$[\mathbf{Z}]\mathbf{v} = \mathbf{f} + \mathbf{g} \tag{8}$$

where, $[\mathbf{Z}]$ is the block diagonal impedance matrix of the P uncoupled sub-structures, $\mathbf{v}$ is the corresponding block vector of velocities, $\mathbf{f}$ is the block vector of applied forces, and $\mathbf{g}$ the block vector of coupling interface forces,

$$[\mathbf{Z}] = \begin{bmatrix} \mathbf{Z^{(1)}} & & & \\ & \mathbf{Z^{(2)}} & & \\ & & \ddots & \\ & & & \mathbf{Z^{(P)}} \end{bmatrix}, \quad \mathbf{v} = \begin{pmatrix} \mathbf{v^{(1)}} \\ \mathbf{v^{(2)}} \\ \vdots \\ \mathbf{v^{(P)}} \end{pmatrix}, \quad \mathbf{f} = \begin{pmatrix} \mathbf{f^{(1)}} \\ \mathbf{f^{(2)}} \\ \vdots \\ \mathbf{f^{(P)}} \end{pmatrix}, \quad \mathbf{g} = \begin{pmatrix} \mathbf{g^{(1)}} \\ \mathbf{g^{(2)}} \\ \vdots \\ \mathbf{g^{(P)}} \end{pmatrix}. \tag{9}$$

The rigid coupling of any two sub-structures is governed by the conditions of compatibility and equilibrium. These may be expressed generally in the form,

$$\mathbf{Bv} = \mathbf{0}, \tag{10}$$

and

$$\mathbf{L^T g} = \mathbf{0}, \tag{11}$$

respectively, where $\mathbf{B}$ and $\mathbf{L}$ represent signed and unsigned Boolean matrices, respectively. Together, equations (8)-(11) are referred to as the three field formulation, and may be solved in a primal or dual manner [1].

The primal solution involves the definition of a unique set of boundary DoFs that belong to the *coupled* assembly. The condition of compatibility is consequently expressed in the form,

$$\mathbf{v} = \mathbf{L}\mathbf{v_C}, \tag{12}$$

where $\mathbf{v_C}$ is the velocity of the coupled assembly. Substitution of equation (12) and (11) into equation (8) leads to an expression for the coupled assembly in the form,

$$\mathbf{Y_C} = \left(\mathbf{LZL^T}\right)^{-1} \tag{13}$$

where $\mathbf{Z}$ is determined from the inverted block diagonal mobility matrix, $\mathbf{Z} = \mathbf{Y^{-1}}$. The above procedure amounts to the summation of impedance matrices of the appropriate dimensions. It is in this way that Finite Element (FE) models are typically assembled. Equation 13 represents the function through which we will propagate uncertainty. In the following section we will derive the appropriate formulae for propagating uncertainty in the *uncoupled* FRF matrix, $\mathbf{Y}$, onto the *coupled* FRF matrix, $\mathbf{Y_C}$.

Note that equation 13 may be used in reverse, i.e. to *decouple* one sub-structure from another. This is achieved by simply adding the *negative* impedance of the residual sub-structure (i.e. the portion of the assembly left once the unknown sub-structure has been removed) to the coupled assembly [28]. For example, the free source FRF $\mathbf{Y_S}$ of a coupled source-receiver assembly is given by

$$\mathbf{Y_S} = \left(\mathbf{L}\begin{bmatrix} \mathbf{Z_C} & \mathbf{0} \\ \mathbf{0} & \mathbf{-Z_R} \end{bmatrix}\mathbf{L^T}\right)^{-1} \tag{14}$$

where $\mathbf{Z_C}$ is the coupled assembly impedance and $\mathbf{-Z_R}$ is the negative receiver impedance. A similar procedure may be performed using the dual formation [28, 29].

As the coupling and decoupling equations are of an identical form, bar the negative impedance, the propagation of uncertainty discussed in the following section will be applicable to both cases. For clarity however, we will consider the coupling case only.

4. Uncertainty Propagation in Dynamic Sub-structuring

In deriving a general framework for the propagation of uncertainty in DS one must not only acknowledge the potential influence of inter-FRF correlations in the uncoupled FRF matrices, but also provide an estimate of the

correlations present between elements of the predicted (coupled) FRF matrix. The quantity of interest is the bivariate covariance matrix,

$$\boldsymbol{\Sigma}_{\mathbf{Y_{Cij}},\mathbf{Y_{Clm}}} = \begin{bmatrix} \sigma_{\Re(Y_{Cij})\Re(Y_{Clm})} & \sigma_{\Re(Y_{Cij})\Im(Y_{Clm})} \\ \sigma_{\Im(Y_{Cij})\Re(Y_{Clk})} & \sigma_{\Im(Y_{Cij})\Im(Y_{Clm})} \end{bmatrix}. \tag{15}$$

The bivariate covariance matrix $\boldsymbol{\Sigma}_{\mathbf{Y_{Cij}},\mathbf{Y_{Clm}}}$ describes generally the statistical relation between the real and imaginary components of any two elements in the coupled FRF matrix $\mathbf{Y_C}$. In this form we are able to estimate the inter-FRF correlation in $\mathbf{Y_C}$ as a result of the uncertainty in $\mathbf{Y}$. Such correlations may be important if the coupled FRFs are to be used in some form of predictive model, for example a VAP.

Assuming that there exists no correlation *between* the uncoupled sub-structures (this is a fair assumption as they are measured independently) the uncertainty present in $\mathbf{Y}$ (i.e. the block diagonal uncoupled FRF matrix) may be described by the covariance matrix $\boldsymbol{\Sigma}_{\mathbf{Y}}$,

$$\boldsymbol{\Sigma}_{\mathbf{Y}} = \begin{bmatrix} \boldsymbol{\Sigma}_{\mathbf{Y^{(1)}}} & \mathbf{0} & \mathbf{0} & \mathbf{0} \\ \mathbf{0} & \boldsymbol{\Sigma}_{\mathbf{Y^{(2)}}} & \mathbf{0} & \mathbf{0} \\ \mathbf{0} & \mathbf{0} & \ddots & \mathbf{0} \\ \mathbf{0} & \mathbf{0} & \mathbf{0} & \boldsymbol{\Sigma}_{\mathbf{Y^{(P)}}} \end{bmatrix} \tag{16}$$

where each sub-structure covariance matrix $\boldsymbol{\Sigma}_{\mathbf{Y^{(P)}}}$ is of the form,

$$\boldsymbol{\Sigma}_{\mathbf{Y^{(P)}}} = \left[\begin{array}{ccc|ccc|c|ccc} \boldsymbol{\Sigma}_{Y_{11},Y_{11}} & \cdots & \boldsymbol{\Sigma}_{Y_{11},Y_{N1}} & \boldsymbol{\Sigma}_{Y_{11},Y_{12}} & \cdots & \boldsymbol{\Sigma}_{Y_{11},Y_{N2}} & \cdots & \boldsymbol{\Sigma}_{Y_{11},Y_{1N}} & \cdots & \boldsymbol{\Sigma}_{Y_{11},Y_{NN}} \\ \vdots & \ddots & \vdots & \vdots & \ddots & \vdots & \cdots & \vdots & \ddots & \vdots \\ \boldsymbol{\Sigma}_{Y_{N1},Y_{11}} & \cdots & \boldsymbol{\Sigma}_{Y_{N1},Y_{N1}} & \boldsymbol{\Sigma}_{Y_{N1},Y_{12}} & \cdots & \boldsymbol{\Sigma}_{Y_{N1},Y_{N2}} & \cdots & \boldsymbol{\Sigma}_{Y_{N1},Y_{1N}} & \cdots & \boldsymbol{\Sigma}_{Y_{N1},Y_{NN}} \\ \hline \boldsymbol{\Sigma}_{Y_{12},Y_{11}} & \cdots & \boldsymbol{\Sigma}_{Y_{12},Y_{N1}} & \boldsymbol{\Sigma}_{Y_{12},Y_{12}} & \cdots & \boldsymbol{\Sigma}_{Y_{12},Y_{N2}} & \cdots & \boldsymbol{\Sigma}_{Y_{12},Y_{1N}} & \cdots & \boldsymbol{\Sigma}_{Y_{12},Y_{NN}} \\ \vdots & \ddots & \vdots & \vdots & \ddots & \vdots & \cdots & \vdots & \ddots & \vdots \\ \boldsymbol{\Sigma}_{Y_{N2},Y_{11}} & \cdots & \boldsymbol{\Sigma}_{Y_{N2},Y_{N1}} & \boldsymbol{\Sigma}_{Y_{N2},Y_{12}} & \cdots & \boldsymbol{\Sigma}_{Y_{N2},Y_{N2}} & \cdots & \boldsymbol{\Sigma}_{Y_{N2},Y_{1N}} & \cdots & \boldsymbol{\Sigma}_{Y_{N2},Y_{NN}} \\ \hline \vdots & \vdots & \vdots & \vdots & \vdots & \vdots & \ddots & \vdots & \vdots & \vdots \\ \hline \boldsymbol{\Sigma}_{Y_{1N},Y_{11}} & \cdots & \boldsymbol{\Sigma}_{Y_{1N},Y_{N1}} & \boldsymbol{\Sigma}_{Y_{1N},Y_{12}} & \cdots & \boldsymbol{\Sigma}_{Y_{1N},Y_{N2}} & \cdots & \boldsymbol{\Sigma}_{Y_{1N},Y_{1N}} & \cdots & \boldsymbol{\Sigma}_{Y_{1N},Y_{NN}} \\ \vdots & \ddots & \vdots & \vdots & \ddots & \vdots & \cdots & \vdots & \ddots & \vdots \\ \boldsymbol{\Sigma}_{Y_{NN},Y_{11}} & \cdots & \boldsymbol{\Sigma}_{Y_{NN},Y_{N1}} & \boldsymbol{\Sigma}_{Y_{NN},Y_{12}} & \cdots & \boldsymbol{\Sigma}_{Y_{NN},Y_{N2}} & \cdots & \boldsymbol{\Sigma}_{Y_{NN},Y_{1N}} & \cdots & \boldsymbol{\Sigma}_{Y_{NN},Y_{NN}} \end{array}\right] \tag{17}$$

with

$$\boldsymbol{\Sigma}_{\mathbf{Y_{ij}},\mathbf{Y_{lm}}} = \begin{bmatrix} \sigma_{\Re(Y_{ij})\Re(Y_{lm})} & \sigma_{\Re(Y_{ij})\Im(Y_{lm})} \\ \sigma_{\Im(Y_{ij})\Re(Y_{lm})} & \sigma_{\Im(Y_{ij})\Im(Y_{lm})} \end{bmatrix}. \tag{18}$$

Note that, although the above covariance matrix will be beneficial in interpreting the uncertainty propagation formulae, an alternative form is used when implementing the framework numerically (see section 5.3).

Recall that the block diagonal structure of $\boldsymbol{\Sigma}_{\mathbf{Y}}$ is due to the uncorrelated nature of any two sub-structures. Similarly, $\boldsymbol{\Sigma}_{\mathbf{Y^{(P)}}}$ will likely possess a block diagonal structure since, under the assumption that correlation only exists between FRFs of shared excitation, $\boldsymbol{\Sigma}_{\mathbf{Y_{ij}},\mathbf{Y_{lm}}}$ will equal $\mathbf{0}$ for $j \neq m$. Furthermore, it is worth noting that the above covariance matrices are readily available from standard measurement data, and require no additional experimental work. It is however necessary that the FRFs corresponding to each individual excitation are recorded alongside their average (see section 5.3).

As per the law of error propagation (see Appendix A), $\boldsymbol{\Sigma}_{\mathbf{Y_{Cij}},\mathbf{Y_{Clm}}}$ and $\boldsymbol{\Sigma}_{\mathbf{Y}}$ are related through the Jacobian of the propagating function such that,

$$\boldsymbol{\Sigma}_{\mathbf{Y_{Cij}},\mathbf{Y_{Clm}}} = \mathbf{J_{ij}}\boldsymbol{\Sigma}_{\mathbf{Y}}\mathbf{J_{lm}^{T}} \tag{19}$$

where $\mathbf{J_{ij}}$ is the Jacobian of the ijth element of the coupled FRF matrix $\mathbf{Y_C}$ with respect to each element of the uncoupled FRF matrix. Note that the law of error propagation is based on a first order Taylor expansion of the propagation function. The propagation function of interest, i.e. the equations for DS, involve matrix inversions and are therefore non-linear. Hence, the law of error propagation is valid only for small uncertainty. In the presence of large uncertainty a more robust approach, for example a Monte-Carlo simulation, may be required.

Since we are considering separately the real and imaginary components of the coupled FRF, the Jacobian $\mathbf{J_{ij}}$ is given as a matrix of partial derivatives with respect to the real and imaginary components of each matrix element,

$$\mathbf{J_{ij}} = \left[\begin{array}{cccc|c|cccc} \frac{\partial \Re(Y_{C_{ij}})}{\partial \Re(Y_{11}^{(1)})} & \frac{\partial \Re(Y_{C_{ij}})}{\partial \Im(Y_{11}^{(1)})} & \cdots & \frac{\partial \Re(Y_{C_{ij}})}{\partial \Re(Y_{NM}^{(1)})} & \frac{\partial \Re(Y_{C_{ij}})}{\partial \Im(Y_{NM}^{(1)})} & \cdots & \frac{\partial \Re(Y_{C_{ij}})}{\partial \Re(Y_{11}^{(P)})} & \frac{\partial \Re(Y_{C_{ij}})}{\partial \Im(Y_{11}^{(P)})} & \cdots & \frac{\partial \Re(Y_{C_{ij}})}{\partial \Re(Y_{NM}^{(P)})} & \frac{\partial \Re(Y_{C_{ij}})}{\partial \Im(Y_{NM}^{(P)})} \\ \frac{\partial \Im(Y_{C_{ij}})}{\partial \Re(Y_{11}^{(1)})} & \frac{\partial \Im(Y_{C_{ij}})}{\partial \Im(Y_{11}^{(1)})} & \cdots & \frac{\partial \Im(Y_{C_{ij}})}{\partial \Re(Y_{NM}^{(1)})} & \frac{\partial \Im(Y_{C_{ij}})}{\partial \Im(Y_{NM}^{(1)})} & \cdots & \frac{\partial \Im(Y_{C_{ij}})}{\partial \Re(Y_{11}^{(P)})} & \frac{\partial \Im(Y_{C_{ij}})}{\partial \Im(Y_{11}^{(P)})} & \cdots & \frac{\partial \Im(Y_{C_{ij}})}{\partial \Re(Y_{NM}^{(P)})} & \frac{\partial \Im(Y_{C_{ij}})}{\partial \Im(Y_{NM}^{(P)})} \end{array}\right] \tag{20}$$

where Y_{Cij} is the ijth element of the coupled FRF matrix, and $Y_{ij}^{(P)}$ is the ijth element of the uncoupled FRF matrix belonging to the Pth sub-structure. To proceed further we must evaluate the above Jacobian.

4.1. Jacobian of the Primal Formulation

We will begin by considering the primal formulation of the DS problem, as illustrated in section 3. Section 4.2 we will briefly cover the dual formulation.

We begin by noting that the complex differential of a matrix inverse is given by (see proposition 3.8 of [30]),

$$d\mathbf{G^{-1}} = -\mathbf{G^{-1}}(d\mathbf{G})\mathbf{G^{-1}} \tag{21}$$

where $\mathbf{G} \in \mathbb{C}^{N\times N}$ is a complex square matrix, whose inverse exists. Using equation 21, the complex differential of $\mathbf{Y_C} = \left(\mathbf{L}\mathbf{Y^{-1}}\mathbf{L^T}\right)^{-1}$ may be written in the form,

$$d\mathbf{Y_C} = -\left(\mathbf{L}\mathbf{Y^{-1}}\mathbf{L^T}\right)^{-1} d\left[\left(\mathbf{L}\mathbf{Y^{-1}}\mathbf{L^T}\right)\right]\left(\mathbf{L}\mathbf{Y^{-1}}\mathbf{L^T}\right)^{-1}. \tag{22}$$

Substituting for the coupled FRF, $\mathbf{Y_C} = \left(\mathbf{L}\mathbf{Y^{-1}}\mathbf{L^T}\right)^{-1}$, whilst noting proposition 3.2 of [30], ($d(\mathbf{GFG}) = \mathbf{G}(d\mathbf{F})\mathbf{G}$ assuming that $\mathbf{G}$ is independent of $\mathbf{F}$), the differential is simplified as so,

$$d\mathbf{Y_C} = -\mathbf{Y_C}\mathbf{L}d\left[\mathbf{Y^{-1}}\right]\mathbf{L^T}\mathbf{Y_C}. \tag{23}$$

Applying again equation 21, the differential takes the form,

$$d\mathbf{Y_C} = \mathbf{Y_C}\mathbf{L}\mathbf{Y^{-1}}(d\mathbf{Y})\,\mathbf{Y^{-1}}\mathbf{L^T}\mathbf{Y_C}. \tag{24}$$

In the above, $d\mathbf{Y_C}$ may be interpreted as the small (complex) change in the coupled FRF matrix, $\mathbf{Y_C}$, given a small change $d\mathbf{Y}$ in the uncoupled FRF matrix, $\mathbf{Y}$. Suppose that the small change in $d\mathbf{Y}$ is limited to a single entry, say Y_{st}. In this case, the differential $d\mathbf{Y}$ may be replaced by the scaled single entry matrix, $\mathbf{P_{st}}dY_{st}$, where $\mathbf{P_{st}}$ is a zero matrix bar the st entry, whose value is one, and dY_{st} is a scalar differential term. Substitution into equation 24 yields,

$$d\mathbf{Y_C} = \left(\mathbf{Y_C}\mathbf{L}\mathbf{Y^{-1}}\mathbf{P_{st}}\mathbf{Y^{-1}}\mathbf{L^T}\mathbf{Y_C}\right)dY_{st}. \tag{25}$$

Finally, the bracketed term in equation 25 is recognised as the partial derivative of $\mathbf{Y_C}$ with respect to the st element of $\mathbf{Y}$,

$$\frac{\partial \mathbf{Y_C}}{\partial Y_{st}} = \mathbf{Y_C}\mathbf{L}\mathbf{Y^{-1}}\mathbf{P_{st}}\mathbf{Y^{-1}}\mathbf{L^T}\mathbf{Y_C}. \tag{26}$$

The Jacobian in equation 20 is defined in terms of the real and imaginary components of $\mathbf{Y_C}$ and $\mathbf{Y}$. As such, equation 26 must now be recast in terms of its real and imaginary components.

Noting that the propagation function $\mathbf{Y_C} = \left(\mathbf{L}\mathbf{Y^{-1}}\mathbf{L^T}\right)^{-1}$ is holomorphic/analytic (i.e. its complex derivative depends only on $\mathbf{Y}$, and not its conjugate), assuming that its inverse matrices exist, the Cauchy-Riemann relations apply to its partial derivatives [31]. Consequently, we have that (see Appendix B),

$$\left[\begin{array}{cc} \frac{\partial \Re(Y_{Cij})}{\partial \Re(Y_{st}^{(P)})} & \frac{\partial \Re(Y_{Cij})}{\partial \Im(Y_{st}^{(P)})} \\ \frac{\partial \Im(Y_{Cij})}{\partial \Re(Y_{st}^{(P)})} & \frac{\partial \Im(Y_{Cij})}{\partial \Im(Y_{st}^{(P)})} \end{array}\right] = \left[\begin{array}{cc} \Re\left(\frac{\partial Y_{Cij}}{\partial Y_{st}^{(P)}}\right) & -\Im\left(\frac{\partial Y_{Cij}}{\partial Y_{st}^{(P)}}\right) \\ \Im\left(\frac{\partial Y_{Cij}}{\partial Y_{st}^{(P)}}\right) & \Re\left(\frac{\partial Y_{Cij}}{\partial Y_{st}^{(P)}}\right) \end{array}\right] = M\left(\mathbf{Y_{Ci:}}\mathbf{L}\mathbf{Y^{-1}}\mathbf{P_{st}}\mathbf{Y^{-1}}\mathbf{L^T}\mathbf{Y_{C:j}}\right) \tag{27}$$

where the function $M(\quad)$ is used to represent the complex matrix mapping operator [26],

$$M(\quad) = \begin{bmatrix} \Re(\quad) & -\Im(\quad) \\ \Im(\quad) & \Re(\quad) \end{bmatrix} \tag{28}$$

and subscripts $_{\mathbf{i}:}$ and $_{:\mathbf{j}}$ denote, respectively, the ith row and jth column of the associated matrices. The Jacobian matrix $\mathbf{J_{ij}}$ is then given by,

$$\mathbf{J_{ij}} = \left[\begin{array}{ccc|c|ccc} M\left(\frac{\partial Y_{Cij}}{\partial Y^{(1)}_{11}}\right) & \cdots & M\left(\frac{\partial Y_{Cij}}{\partial Y^{(1)}_{NM}}\right) & \cdots & M\left(\frac{\partial Y_{Cij}}{\partial Y^{(P)}_{11}}\right) & \cdots & M\left(\frac{\partial Y_{Cij}}{\partial Y^{(P)}_{NM}}\right) \end{array} \right]. \tag{29}$$

Together, equations 19, 27 and 29 allow the propagation of complex and correlated uncertainty through a primal DS procedure.[3] Although based on a primal formulation of the DS problem, as was discussed in [5], the proposed propagation framework is valid for sub-structured FRFs in general, regardless of the way in which they are coupled as the underlying physics are the same. Nevertheless, if a dual formulation is preferred, the bivariate Jacobian element of equation 27 may be replaced by that of equation 36. Note that in either case the Jacobians need only evaluated for the non-zero entries of $\mathbf{Y}$. Similarly, if the covariance matrix of a particular substructure, $\mathbf{\Sigma_{Y^{(p)}}}$, has a block diagonal structure, those elements with 0 covariance need not be included in the propagation.

For non-square sub-structure matrices (i.e. where additional force/response-only DoFs are included) it is important to note that the primal formulation presented above is not applicable. In the primal formulation a non-square FRF matrix would require the inverse operations to be replaced by the pseudo-inverse, whose complex derivative is *not* holomorphic. As such the Jacobian derived in equation 29 would no longer be correct. Whilst the propagation of uncertainty through a pseduo-inverse was demonstrated in [10], the additional term introduced complicates the formulation of a primal Jacobian (due to the double inversion), and so is not considered in this work. However, noting that in the dual formulation (see section 4.2) the term $\mathbf{BYB^T}$ performs a collocation of *interface* DoFs, the resultant matrix is by definition square, and thus requires only a standard matrix inversion. In conclusion, the non-square case cannot be easily handled using the above primal formulation, although it may be treated using the dual formulation. Hence a corresponding derivation with the dual formulation will now be given.

4.2. Jacobian of the Dual Formulation

In what follows we will derive the bivariate Jacobian element associated with a dual formulation of the DS problem. This Jacobian must be used in place of the primal formulation leading to equation 27 if non-square FRF matrices are present.

As per the dual formulation, the coupled FRF is given by,

$$\mathbf{Y_C} = \mathbf{Y} - \mathbf{YB^T}\left(\mathbf{BYB^T}\right)^{-1}\mathbf{BY}, \tag{30}$$

where $\mathbf{B}$ is a signed Boolean localisation matrix. The details regarding the formulation of equation 30, and the construction of $\mathbf{B}$ can be found in [1].

We are interested in the derivative of equation 30 with respect to the real and imaginary components of each matrix element. The derivation follows similar steps to that of the primal formulation. We begin by considering the complex differential of $\mathbf{Y_C}$ in the form,

$$d\mathbf{Y_C} = d\mathbf{Y} - d\left(\mathbf{YB^T}\left(\mathbf{BYB^T}\right)^{-1}\mathbf{BY}\right). \tag{31}$$

Application of the chain rule to the second right hand side term, whilst noting proposition 3.2 of [30], ($d\left(\mathbf{GFG}\right) = \mathbf{G}\left(d\mathbf{F}\right)\mathbf{G}$ assuming that $\mathbf{G}$ is independent of $\mathbf{F}$), yields,

$$d\mathbf{Y_C} = d\mathbf{Y} - \left[\{d\mathbf{Y}\}\mathbf{B^T}\left(\mathbf{BYB^T}\right)^{-1}\mathbf{BY} + \mathbf{YB^T}\left\{d\left(\mathbf{BYB^T}\right)^{-1}\right\}\mathbf{BY} + \mathbf{YB^T}\left(\mathbf{BYB^T}\right)^{-1}\mathbf{B}\{d\mathbf{Y}\}\right]. \tag{32}$$

[3] A straightforward numerical implementation of this framework is given in section 5.

Recalling that the complex differential of a matrix inverse is given by $d\mathbf{G^{-1}} = -\mathbf{G^{-1}}(d\mathbf{G})\mathbf{G^{-1}}$ [30], the above differential becomes,

$$d\mathbf{Y_C} = d\mathbf{Y} - \left[\{d\mathbf{Y}\}\mathbf{B^T}\left(\mathbf{BYB^T}\right)^{-1}\mathbf{BY} - \mathbf{YB^T}\left(\mathbf{BYB^T}\right)^{-1}\left(\mathbf{B}\{d\mathbf{Y}\}\mathbf{B^T}\right)\left(\mathbf{BYB^T}\right)^{-1}\mathbf{BY} + \mathbf{YB^T}\left(\mathbf{BYB^T}\right)^{-1}\mathbf{B}\{d\mathbf{Y}\}\right]. \quad (33)$$

Now, from equation 33 the differential $d\mathbf{Y_C}$ may be interpreted as the small (complex) change in the coupled mobility matrix, given the small change $d\mathbf{Y}$ in the uncoupled mobility matrix. Suppose that the small change in $d\mathbf{Y}$ is limited to a single entry, say Y_{st}. In such a case, the differential $d\mathbf{Y}$ may be replaced by the scaled single entry matrix, $\mathbf{P_{st}}dY_{st}$. Substitution into equation 33 yields,

$$d\mathbf{Y_C} = \left[\mathbf{P_{st}} - \mathbf{P_{st}B^T}\left(\mathbf{BYB^T}\right)^{-1}\mathbf{BY} + \mathbf{YB^T}\left(\mathbf{BYB^T}\right)^{-1}\left(\mathbf{BP_{st}B^T}\right)\left(\mathbf{BYB^T}\right)^{-1}\mathbf{BY} - \mathbf{YB^T}\left(\mathbf{BYB^T}\right)^{-1}\mathbf{BP_{st}}\right]dY_{st}. \quad (34)$$

The square bracketed term in the above expression represents the complex derivative of the coupled FRF matrix $\mathbf{Y_C}$, with respect to the st element of the uncoupled FRF matrix, Y_{st}. The derivative of the ijth element is thus given by,

$$\left(\frac{\partial \mathbf{Y_C}}{\partial Y_{st}}\right)_{ij} = \left[\mathbf{P_{st}} - \mathbf{P_{st}B^T}\left(\mathbf{BYB^T}\right)^{-1}\mathbf{BY} + \mathbf{YB^T}\left(\mathbf{BYB^T}\right)^{-1}\mathbf{BP_{st}B^T}\left(\mathbf{BYB^T}\right)^{-1}\mathbf{BY} - \mathbf{YB^T}\left(\mathbf{BYB^T}\right)^{-1}\mathbf{BP_{st}}\right]_{ij}. \quad (35)$$

Noting that the dual formulation (equation 30) is also holomorphic, a bivariate element of its Jacobian is given by,

$$\begin{bmatrix} \frac{\partial \Re(Y_{Cij})}{\partial \Re(Y_{st}^{(P)})} & \frac{\partial \Re(Y_{Cij})}{\partial \Im(Y_{st}^{(P)})} \\ \frac{\partial \Im(Y_{Cij})}{\partial \Re(Y_{st}^{(P)})} & \frac{\partial \Im(Y_{Cij})}{\partial \Im(Y_{st}^{(P)})} \end{bmatrix} = M\left(\left[\mathbf{P_{st}} - \mathbf{P_{st}B^T}\left(\mathbf{BYB^T}\right)^{-1}\mathbf{BY} + \mathbf{YB^T}\left(\mathbf{BYB^T}\right)^{-1}\mathbf{BP_{st}B^T}\left(\mathbf{BYB^T}\right)^{-1}\mathbf{BY} - \mathbf{YB^T}\left(\mathbf{BYB^T}\right)^{-1}\mathbf{BP_{st}}\right]_{ij}\right) \quad (36)$$

where $M(\quad)$ is once again the complex matrix mapping operator. Equation 36 may readily be substituted into equation 19 and 20 to yield an uncertainty propagation framework in terms of the dual formulation. For square FRF matrices, the above would, in theory, provide an identical propagation of uncertainty as the primal approach presented through section 4.1.

4.3. Evaluation of the Primal Jacobian - An Algebraic Example

In what follows we will examine the mechanics of the primal Jacobian (equation 26) so as to better understand the process of uncertainty propagation. To do so we will make use of the simple two sub-structure assembly shown in figure 1, although the conclusions drawn will apply more generally to assemblies made up of an arbitrary number of sub-structures.

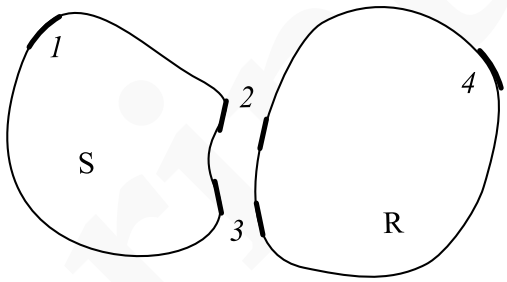

Figure 1: Schematic of the Source-Receiver assembly used in the algebraic example if the Jacobian construction.

A source (S) and receiver (R) sub-structure are rigidly coupled at two boundary DoFs, labelled 2 and 3. An additional internal DoF is also included on each sub-structure, labelled 1 and 4, respectively. The *uncoupled* assembly

impedance matrix is given by,

$$\mathbf{Z} = \left[\begin{array}{ccc|ccc} Z_{S11} & Z_{S12} & Z_{S13} & 0 & 0 & 0 \\ Z_{S21} & Z_{S22} & Z_{S23} & 0 & 0 & 0 \\ Z_{S31} & Z_{S32} & Z_{S33} & 0 & 0 & 0 \\ \hline 0 & 0 & 0 & Z_{R22} & Z_{R23} & Z_{R24} \\ 0 & 0 & 0 & Z_{R32} & Z_{R33} & Z_{R34} \\ 0 & 0 & 0 & Z_{R42} & Z_{R43} & Z_{R44} \end{array}\right] = \mathbf{Y^{-1}}. \tag{37}$$

The corresponding Boolean coupling matrix $\mathbf{L}$ is,

$$\mathbf{L} = \begin{bmatrix} 1 & 0 & 0 & 0 & 0 & 0 \\ 0 & 1 & 0 & 1 & 0 & 0 \\ 0 & 0 & 1 & 0 & 1 & 0 \\ 0 & 0 & 0 & 0 & 0 & 1 \end{bmatrix}. \tag{38}$$

The mobility of the *coupled* structure is consequently given by,

$$\mathbf{Y_C} = \mathbf{Z_C^{-1}} = \begin{bmatrix} Z_{S11} & Z_{S12} & Z_{S13} & 0 \\ Z_{S21} & Z_{S22} + Z_{R22} & Z_{S23} + Z_{R23} & Z_{R24} \\ Z_{S31} & Z_{S32} + Z_{R32} & Z_{S33} + Z_{R33} & Z_{R34} \\ 0 & Z_{R42} & Z_{R43} & Z_{R44} \end{bmatrix}^{-1} \tag{39}$$

where it is noted that the (impedance of) internal DoFs (1 and 4) are unaffected by structural coupling (i.e. $Z_{C11} = Z_{S11}$, $Z_{C12} = Z_{S12}$, $Z_{C13} = Z_{S13}$ and $Z_{C44} = Z_{R44}$, $Z_{C42} = Z_{R42}$, $Z_{C43} = Z_{R43}$, as with their reciprocal values).

Given the above assembly, we are concerned with the evaluation of the Jacobian,

$$\frac{\partial Y_{Cij}}{\partial Y_{st}} = \left(\mathbf{Y_C L Y^{-1} P_{st} Y^{-1} L^T Y_C}\right)_{ij} \tag{40}$$

which describes the propagation of uncertainty from the uncoupled FRF element, Y_{st}, onto the coupled FRF, Y_{Cij}.

Let us examine equation 40 beginning with the left side product, $\mathbf{Y_C L Y^{-1}}$. The Boolean coupling matrix $\mathbf{L}$, when pre-multiplying $\mathbf{Y^{-1}}$, enforces equilibrium among the collocated boundary DoFs (2 and 3) such that,

$$\begin{bmatrix} 1 & 0 & 0 & 0 & 0 & 0 \\ 0 & 1 & 0 & 1 & 0 & 0 \\ 0 & 0 & 1 & 0 & 1 & 0 \\ 0 & 0 & 0 & 0 & 0 & 1 \end{bmatrix} \left[\begin{array}{ccc|ccc} Z_{S11} & Z_{S12} & Z_{S13} & 0 & 0 & 0 \\ Z_{S21} & Z_{S22} & Z_{S23} & 0 & 0 & 0 \\ Z_{S31} & Z_{S32} & Z_{S33} & 0 & 0 & 0 \\ \hline 0 & 0 & 0 & Z_{R22} & Z_{R23} & Z_{R24} \\ 0 & 0 & 0 & Z_{R32} & Z_{R33} & Z_{R34} \\ 0 & 0 & 0 & Z_{R42} & Z_{R43} & Z_{R44} \end{array}\right] = \left[\begin{array}{ccc|ccc} Z_{S11} & Z_{S12} & Z_{S13} & 0 & 0 & 0 \\ \hline Z_{S21} & Z_{S22} & Z_{S23} & Z_{R22} & Z_{R23} & Z_{R24} \\ Z_{S31} & Z_{S32} & Z_{S33} & Z_{R32} & Z_{R33} & Z_{R34} \\ \hline 0 & 0 & 0 & Z_{R42} & Z_{R43} & Z_{R44} \end{array}\right]. \tag{41}$$

Given that the impedance of an internal DoF is unaffected by structural coupling (i.e. the columns of $\mathbf{LY^{-1}}$ associated with internal DoFs are identical to those of $\mathbf{Y_C^{-1}}$), pre-multiplication by $\mathbf{Y_C}$ will return a matrix whose columns are either single entry, or non-zero vectors, depending on whether the associated DoF is an internal or boundary one, respectively. For the example assembly considered pre-multiplication yields,

$$\begin{bmatrix} Y_{C11} & Y_{C12} & Y_{C13} & Y_{C14} \\ Y_{C21} & Y_{C22} & Y_{C23} & Y_{C24} \\ Y_{C31} & Y_{C32} & Y_{C33} & Y_{C34} \\ Y_{C41} & Y_{C42} & Y_{C43} & Y_{C44} \end{bmatrix} \left[\begin{array}{ccc|ccc} Z_{S11} & Z_{S12} & Z_{S13} & 0 & 0 & 0 \\ \hline Z_{S21} & Z_{S22} & Z_{S23} & Z_{R22} & Z_{R23} & Z_{R24} \\ Z_{S31} & Z_{S32} & Z_{S33} & Z_{R32} & Z_{R33} & Z_{R34} \\ \hline 0 & 0 & 0 & Z_{R42} & Z_{R43} & Z_{R44} \end{array}\right] = \begin{bmatrix} 1 & * & * & * & * & 0 \\ 0 & * & * & * & * & 0 \\ 0 & * & * & * & * & 0 \\ 0 & * & * & * & * & 1 \end{bmatrix} \tag{42}$$

where $*$ indicates a non-zero value. These non-zero entries arise from the fact that the columns of $\mathbf{LY^{-1}}$ associated with the boundary DoFs remain uncoupled (see equation 41). The magnitude of the non-zero entries will depend on the impedance of the associated sub-structure. A stiffer sub-structure will generally lead to greater non-zero values and consequently an amplification of the propagated uncertainty.

Following a similar procedure for the right side product, $\mathbf{Y}^{-1}\mathbf{L}^{\mathbf{T}}\mathbf{Y}_{\mathbf{C}}$, we get,

$$\left[\begin{array}{c|ccc} Z_{S11} & Z_{S12} & Z_{S13} & 0 \\ Z_{S21} & Z_{S22} & Z_{S23} & 0 \\ Z_{S31} & Z_{S32} & Z_{S33} & 0 \\ \hline 0 & Z_{R22} & Z_{R23} & Z_{R24} \\ 0 & Z_{R32} & Z_{R33} & Z_{R34} \\ 0 & Z_{R42} & Z_{R43} & Z_{R44} \end{array}\right] \begin{bmatrix} Y_{C11} & Y_{C12} & Y_{C13} & Y_{C14} \\ Y_{C21} & Y_{C22} & Y_{C23} & Y_{C24} \\ Y_{C31} & Y_{C32} & Y_{C33} & Y_{C34} \\ Y_{C41} & Y_{C42} & Y_{C43} & Y_{C44} \end{bmatrix} = \begin{bmatrix} 1 & 0 & 0 & 0 \\ * & * & * & * \\ * & * & * & * \\ * & * & * & * \\ * & * & * & * \\ 0 & 0 & 0 & 1 \end{bmatrix}. \tag{43}$$

Substituting the above into equation 40, whilst considering all elements of $\mathbf{Y}_{\mathbf{C}}$, we arrive at,

$$\frac{\partial \mathbf{Y}_{\mathbf{C}}}{\partial Y_{st}} = \begin{bmatrix} 1 & * & * & * & * & 0 \\ 0 & * & * & * & * & 0 \\ 0 & * & * & * & * & 0 \\ 0 & * & * & * & * & 1 \end{bmatrix} [\mathbf{P_{st}}] \begin{bmatrix} 1 & 0 & 0 & 0 \\ * & * & * & * \\ * & * & * & * \\ * & * & * & * \\ * & * & * & * \\ 0 & 0 & 0 & 1 \end{bmatrix}. \tag{44}$$

Equation 44 illustrates how an uncertainty in the st entry of the uncoupled FRF matrix $\mathbf{Y}$ propagates onto the each element of coupled FRF matrix $\mathbf{Y}_{\mathbf{C}}$.

Noting that the single entry matrix $\mathbf{P_{st}}$ performs an outer product between column s and row t of its left and right hand matrices, respectively, the structure of the resultant matrix is seen to depend on which uncoupled FRF, Y_{st}, is considered. By analysing the outer product, given a particular st, we are able to track the uncertainty of an FRF as it propagates through the DFSS procedure. From this we are able to make the following conclusions.

1) Selection of an internal-internal FRF will lead to an outer product between two single entry vectors. Consequently, the associated uncertainty will not propagate beyond the internal-internal FRF itself. For example, an uncertainty in Y_{S11} will propagate according to,

$$\frac{\partial \mathbf{Y}_{\mathbf{C}}}{\partial Y_{11}} = \begin{bmatrix} 1 & * & * & * & * & 0 \\ 0 & * & * & * & * & 0 \\ 0 & * & * & * & * & 0 \\ 0 & * & * & * & * & 1 \end{bmatrix} [\mathbf{P_{11}}] \begin{bmatrix} 1 & 0 & 0 & 0 \\ * & * & * & * \\ * & * & * & * \\ * & * & * & * \\ * & * & * & * \\ 0 & 0 & 0 & 1 \end{bmatrix} = \begin{bmatrix} 1 & 0 & 0 & 0 \\ 0 & 0 & 0 & 0 \\ 0 & 0 & 0 & 0 \\ 0 & 0 & 0 & 0 \end{bmatrix} \tag{45}$$

which is non-zero only in the 11 entry, i.e. an uncertainty in Y_{S11} will influence only Y_{C11}.

2) Selection of an internal-boundary FRF will lead to an outer product between a single entry, and a non-zero vector. The resultant matrix will have a single non-zero row or column (depending on st). Consequently, the associated uncertainty will propagate through to all FRFs that share the same internal DoF as a response or excitation (depending on st). For example, an uncertainty in Y_{S13} will propagate according to,

$$\frac{\partial \mathbf{Y}_{\mathbf{C}}}{\partial Y_{13}} = \begin{bmatrix} 1 & * & * & * & * & 0 \\ 0 & * & * & * & * & 0 \\ 0 & * & * & * & * & 0 \\ 0 & * & * & * & * & 1 \end{bmatrix} [\mathbf{P_{13}}] \begin{bmatrix} 1 & 0 & 0 & 0 \\ * & * & * & * \\ * & * & * & * \\ * & * & * & * \\ * & * & * & * \\ 0 & 0 & 0 & 1 \end{bmatrix} = \begin{bmatrix} * & * & * & * \\ 0 & 0 & 0 & 0 \\ 0 & 0 & 0 & 0 \\ 0 & 0 & 0 & 0 \end{bmatrix} \tag{46}$$

where the non-zero entries correspond to: Y_{C11}, Y_{C12}, Y_{C13} and Y_{C14} (i.e. they share the internal DoF as a

response position). Similarly, an uncertainty in Y_{S31} will propagate according to,

$$\frac{\partial \mathbf{Y_C}}{\partial Y_{31}} = \begin{bmatrix} 1 & * & * & * & * & 0 \\ 0 & * & * & * & * & 0 \\ 0 & * & * & * & * & 0 \\ 0 & * & * & * & * & 1 \end{bmatrix} [\mathbf{P_{31}}] \begin{bmatrix} 1 & 0 & 0 & 0 \\ * & * & * & * \\ * & * & * & * \\ * & * & * & * \\ * & * & * & * \\ 0 & 0 & 0 & 1 \end{bmatrix} = \begin{bmatrix} * & 0 & 0 & 0 \\ * & 0 & 0 & 0 \\ * & 0 & 0 & 0 \\ * & 0 & 0 & 0 \end{bmatrix} \tag{47}$$

where the non-zero entries correspond to: Y_{C11}, Y_{C21}, Y_{C31} and Y_{C41} (i.e. they share the internal DoF as an excitation position).

3) Selection of a boundary-boundary FRF will lead to an outer product between two non-zero vectors. The resultant matrix will be fully populated. Consequently, the associated uncertainty will propagate through to *all* FRFs. For example, an uncertainty in Y_{S23} will propagate according to,

$$\frac{\partial \mathbf{Y_C}}{\partial Y_{23}} = \begin{bmatrix} 1 & * & * & * & * & 0 \\ 0 & * & * & * & * & 0 \\ 0 & * & * & * & * & 0 \\ 0 & * & * & * & * & 1 \end{bmatrix} [\mathbf{P_{23}}] \begin{bmatrix} 1 & 0 & 0 & 0 \\ * & * & * & * \\ * & * & * & * \\ * & * & * & * \\ * & * & * & * \\ 0 & 0 & 0 & 1 \end{bmatrix} = \begin{bmatrix} * & * & * & * \\ * & * & * & * \\ * & * & * & * \\ * & * & * & * \end{bmatrix}. \tag{48}$$

The above results are in agreement with those of Voormeeren et al. [5]. However, the proposed framework (outlined through section 4) considers not only the propagation of variance in the uncoupled FRFs (as in [5]), but also their covariance. As such, it is important to consider the necessary conditions under which covariance is propagated.

The variance in an element of the uncoupled FRF matrix is propagated onto the variance of a coupled FRF by the square of the appropriate Jacobian term.

$$\left(\frac{\partial Y_{Cij}}{\partial Y_{st}}\right)^2 \sigma_{Y_{st}Y_{st}} \rightarrow \sigma_{Y_{Cij}Y_{Cij}} \tag{49}$$

The covariance between two elements of the uncoupled FRF matrix, on the other hand, is propagated by two different Jacobian terms, one associated with each of the correlated FRFs.

$$\frac{\partial Y_{Cij}}{\partial Y_{st}} \frac{\partial Y_{Cij}}{\partial Y_{lm}} \sigma_{Y_{st}Y_{lm}} \rightarrow \sigma_{Y_{Cij}Y_{Cij}} \tag{50}$$

In order for the uncoupled covariance $\sigma_{Y_{st}Y_{lm}}$ to propagate, both Jacobian terms must be non-zero. As an example, the covariance between Y_{S13} and Y_{S23}, $\sigma_{Y_{S13},Y_{S23}}$, which will be non-zero on the basis of operator uncertainty (due to their shared excitation), will not propagate onto the uncertainty in Y_{C44}, as its derivative with respect to Y_{S13} is 0, $\frac{\partial Y_{C44}}{\partial Y_{S13}} = 0$ (see equation 46). From the above we are able to draw the following conclusions.

1) The covariance between any two uncoupled internal-internal FRFs will only propagate onto the variance of and the covariance between the same two FRFs on the coupled structure.

2) The covariance between any two uncoupled boundary-boundary FRFs will influence the variance of and the covariance between all coupled FRFs of the assembled structure.

3) The remaining covariances (i.e between internal-internal, boundary-boundary, and internal-boundary FRFs) will influence the variance and covariance of the coupled FRFs in different proportions according to the relative position of the uncoupled FRFs considered.

The above remarks suggest that, if neglected, the presence of inter-FRF correlation in any sub-structure could lead to an inaccurate estimate of uncertainty in all coupled FRFs. By including such covariance terms in the proposed framework, we are able to avoid such errors.

4.4. Additional Remarks

Before proceeding a few more general remarks are warranted. Most importantly, the law of error propagation, as used in the above formulation, is based on a first order expansion of the propagation function (see Appendix A). As such, it is valid only in the presence of small levels of uncertainty. For this reason care must be taken in the vicinity of sharp resonances, where small shifts in frequency can lead to large changes in amplitude. A second order formulation could be established by extending equations A.3 and A.4 to include second order derivatives (this was done in [5] for the dual formulation in the case of uncorrelated uncertainty). However, the resultant expressions become unwieldy. This is particularly so in the presence of operator (i.e correlated) uncertainty, as one cannot neglect the joint variability between FRF elements. In the presence of large uncertainty it is suggested that a Monte-Carlo propagation be performed.

Regarding the sensitivity of coupled FRF uncertainty to the dynamics of the uncoupled sub-structures, it was shown in the above example that stiffer (higher impedance) substructures will tend to contribute more to the overall uncertainty than less stiff ones (assuming a similar initial uncertainty). This suggests that a greater degree of uncertainty may be tolerated in flexible/resilient components than those stiffer if the aim is to fit within some predefined level of acceptable uncertainty.

Furthermore, similarly to the formulation presented in [5], from equation 40 it can be seen that the uncertainties present in the uncoupled FRFs are magnified at resonance (of the coupled assembly) by the outermost FRF terms of the Jacobian. Further amplification will occur at the maxima regions of the uncoupled sub-structure's impedance due to the inverse (uncoupled) FRF term, $\mathbf{Y^{-1}}$. Unlike the resonance amplification, these maxima will differ in frequency among the entries of $\mathbf{Y^{-1}}$. This amplification is governed according to the matrix $\mathbf{P_{st}}$, which selects the appropriate row and column of $\mathbf{Y^{-1}}$. In each case, the presence of low damping will likely lead to a greater propagation of uncertainty.

Also, as discussed in section 3, the proposed framework is valid in a sub-structure decoupling context, as the Jacobian is of the same form. The only modification required would be the negation of the residual impedance matrix in the $\mathbf{Y^{-1}}$ term, and the replacement of $\mathbf{Y_C}$ with the appropriate decoupled FRF matrix.

Furthermore, the proposed framework it is not restricted to random or uncertain FRF matrices. For example, if a deterministic substructure (say from a numerical model) were to be included, its covariance matrix would simply be the zero matrix, $\mathbf{\Sigma_{Y^{(Det)}}} = \mathbf{0}$. In this case, the proposed framework would estimate the influence of the experimental uncertainty on the deterministic components of the coupled model. Moreover, there is no requirement that the covariance matrices used be determined experimentally. If a numerical sub-structure was considered, an appropriate covariance matrix may be obtained for example, through a Monte-Carlo simulation, if the computational resources were available.

As a final remark, it is worth considering the size of the resultant expressions obtained when using the proposed framework. As an example, consider two substructures A and B, each characterised by n DoFs. Their full FRF matrices will be of dimensions $n \times n$. Consequently, their covariance matrices will each be $2n^2 \times 2n^2$. Together, the uncoupled covariance matrix (obtained by block diagonalising the sub-structure covariance matrices) is of dimensions $4n^2 \times 4n^2$. Say that A and B are coupled rigidly at m DoFs using the primal procedure, the coupled assembly would be characterised by the $(2n-m)\times(2n-m)$ FRF matrix, and its uncertainty by a $2(2n-m)^2 \times 2(2n-m)^2$ covariance matrix. For consistency the Jacobian matrix used in the propagation of uncertainty must be of dimensions $2(2n-m)^2 \times 4n^2$. For a typical case, say $n = 5$ and $m = 4$ (e.g. 4 footed vibration source coupled to receiver, with additional remote DoF retained on each side), the propagation framework would require a Jacobian matrix of dimension 72×100 and an uncoupled covariance matrix of dimensions 100×100. Although large by conventional experimental standards, these matrices are easily handled by modern computers. Furthermore, the only (minimal) additional measurement effort required in their construction would be to retain results from individual hammer hits (for the estimation of the FRF covariance) rather than averaging prior to analysis. That said, their construction is potentially highly time consuming and prone to error. For this reason we are also concerned with efficient and rigorous methods for constructing the required covariance and Jacobian matrices. This will be the topic of the following section.

5. Numerical Implementation of the Uncertainty Propagation Framework

The primal and dual formulations of DS considered in this work are formulated in the frequency domain. Consequently, a frequency-by-frequency evaluation of uncertainty is performed. For realistic levels of complexity (i.e.

multiple DoFs per sub-structure), the propagation framework may, if not implemented correctly, take considerable time to run. To reduce computation effort, and limit the opportunity for coding errors, we are interested in an efficient and rigorous construction of the primal and dual Jacobian matrices, as represented by equation 27 and 36, respectively. In what follows we will derive concise expressions for the *complete* Jacobian matrices, which may readily be implemented into numerical code. The construction of an appropriate covariance matrix will also be discussed.

5.1. Primal Formulation

We begin by recalling the vectorisation operator, vec( ), which stacks the columns of the associated matrix such that, given $\mathbf{A} \in \mathbb{C}^{N\times M}$, $\text{vec}(\mathbf{A}) = \mathbf{a} \in \mathbb{C}^{NM\times 1}$. Noting lemma 2.11 from [30],

$$\text{vec}(\mathbf{ABC}) = (\mathbf{C}^{\mathbf{T}} \otimes \mathbf{A})\text{vec}(\mathbf{B}) \tag{51}$$

where $\otimes$ denotes the Kronecker product (see definition 2.6 of [30]), the vectorised complex derivative of $\mathbf{Y_C}$ with respect to the *st* element of $\mathbf{Y}$ (see equation 26) is given by,

$$\text{vec}\left(\mathbf{Y_C L Y^{-1} P_{st} Y^{-1} L^T Y_C}\right) = \left(\mathbf{Y^{-1} L^T Y_C}\right)^{\mathbf{T}} \otimes \left(\mathbf{Y_C L Y^{-1}}\right)\text{vec}(\mathbf{P_{st}}). \tag{52}$$

The above expression yields a column vector whose entries are the complex derivatives of $\mathbf{Y_C}$ with respect to the *st* element of $\mathbf{Y}$ only.

Noting that as one cycles through the *st* elements of $\mathbf{P_{st}}$, $\text{vec}(\mathbf{P_{st}})$ represents a unit vector whose index increases with each step. Clearly, by arranging each $\text{vec}(\mathbf{P_{st}})$ as the columns of a matrix we arrive at the identity matrix $\mathbf{I}$. As such,

$$\left(\mathbf{Y^{-1} L^T Y_C}\right)^{\mathbf{T}} \otimes \left(\mathbf{Y_C L Y^{-1}}\right)\text{vec}(\mathbf{P_{st}}) \rightarrow \left(\mathbf{Y^{-1} L^T Y_C}\right)^{\mathbf{T}} \otimes \left(\mathbf{Y_C L Y^{-1}}\right). \tag{53}$$

In doing so, the right hand term in the above equation yields a matrix whose columns represent the derivatives of $\mathbf{Y_C}$ with respect to each element of $\mathbf{Y}$ (including its zero entries). Consequently, the full primal Jacobian matrix is given by,

$$\mathbf{J} = M\left(\left(\mathbf{Y^{-1} L^T Y_C}\right)^{\mathbf{T}} \otimes \left(\mathbf{Y_C L Y^{-1}}\right)\right) \tag{54}$$

where the complex matrix mapping, $M(\ )$, defined in equation 28, is applied element-wise. Finally, the full covariance matrix of the coupled system is given, conveniently, by,

$$\mathbf{\Sigma_{Y_C}} = \mathbf{J}\mathbf{\Sigma_Y}\mathbf{J}^{\mathbf{T}}. \tag{55}$$

Equation 54 and 55 provide a straightforward numerical implementation of the proposed uncertainty propagation framework. Note that equation 55 requires the covariance matrix $\mathbf{\Sigma_Y}$ to be constructed such that it is compatible with the Jacobian matrix $\mathbf{J}$. This will be discussed in section 5.3.

5.2. Dual Formulation

For the dual formulation we note that the vectorised complex derivative (see equation 35) may be written as the sum of its vectorised terms as follows,

$$\begin{aligned}&\text{vec}\left(\mathbf{P_{st}} - \mathbf{P_{st}B^T}\left(\mathbf{BYB^T}\right)^{-1}\mathbf{BY} + \mathbf{YB^T}\left(\mathbf{BYB^T}\right)^{-1}\mathbf{BP_{st}B^T}\left(\mathbf{BYB^T}\right)^{-1}\mathbf{BY} - \mathbf{YB^T}\left(\mathbf{BYB^T}\right)^{-1}\mathbf{BP_{st}}\right) = \\ &\text{vec}\left(\mathbf{P_{st}}\right) - \text{vec}\left(\mathbf{P_{st}B^T}\left(\mathbf{BYB^T}\right)^{-1}\mathbf{BY}\right) + \text{vec}\left(\mathbf{YB^T}\left(\mathbf{BYB^T}\right)^{-1}\mathbf{BP_{st}B^T}\left(\mathbf{BYB^T}\right)^{-1}\mathbf{BY}\right) - \text{vec}\left(\mathbf{YB^T}\left(\mathbf{BYB^T}\right)^{-1}\mathbf{BP_{st}}\right).\end{aligned} \tag{56}$$

Making use of equation 51 (whilst substituting the identity matrix for $\mathbf{A}$ and $\mathbf{C}$ when required), and following a similar procedure as with the primal case, we arrive at the full dual Jacobian matrix,

$$\mathbf{J} = M\left(\mathbf{I} - \left[\left(\mathbf{B^T}\left(\mathbf{BYB^T}\right)^{-1}\mathbf{BY}\right)^{\mathbf{T}} \otimes \mathbf{I}\right] + \left[\left(\mathbf{B^T}\left(\mathbf{BYB^T}\right)^{-1}\mathbf{BY}\right)^{\mathbf{T}} \otimes \mathbf{YB^T}\left(\mathbf{BYB^T}\right)^{-1}\mathbf{B}\right] - \left[\mathbf{I} \otimes \mathbf{YB^T}\left(\mathbf{BYB^T}\right)^{-1}\mathbf{B}\right]\right) \tag{57}$$

where the complex matrix mapping is again applied element-wise.

Equation 57 may be used in place of equation 54 to determine the full covariance matrix of the coupled system based on the dual formulation. Note however, the resultant covariance matrix $\mathbf{\Sigma_{Y_C}}$ will be larger than that obtained by the primal method, as the dual formulation retains all DoFs belonging to the uncoupled sub-structures.

5.3. Uncoupled Covariance Matrix

It is important that the uncoupled covariance matrix $\mathbf{\Sigma_Y}$ used in the above implementation be consistent with the Jacobian matrices given by equation 54 and 57. Noting that the Jacobians were obtained by horizontally aligning all vec($\mathbf{P_{st}}$) vectors such that they formed an identity matrix, $\mathbf{\Sigma_Y}$ must be built by stacking the *columns* of the uncoupled FRF matrix $\mathbf{Y}$ (including the zero entries), and calculating the associated covariance matrix. As we have assumed independence between the uncoupled sub-structures, this covariance matrix will be sparse. For large systems the sub-structure covariance matrices may be calculated separately and their elements assigned appropriately to those of the uncoupled covariance matrix $\mathbf{\Sigma_Y}$.

Given the uncoupled (i.e. block diagonal) FRF matrix, $\mathbf{Y}$, whose columns are each measured E times, a covariance matrix is obtained by first vectorising, each matrix 'realisation' as so,

$$\hat{\mathbf{Y}} = \left[\begin{array}{cccc} M_v\left(\mathrm{Vec}[\mathbf{Y}_{(1)}]\right) & M_v\left(\mathrm{Vec}[\mathbf{Y}_{(2)}]\right) & \cdots & M_v\left(\mathrm{Vec}[\mathbf{Y}_{(E)}]\right) \end{array} \right] \tag{58}$$

where the operator,

$$M_v(A) = \left(\begin{array}{c} \Re(A) \\ \Im(A) \end{array} \right) \tag{59}$$

is applied element wise, and $\mathbf{Y}_{(E)}$ represents the FRF matrix constructed using the Eth measurement of each column. The covariance matrix is then calculated using the standard formula,

$$\mathbf{\Sigma_Y} = \frac{1}{E}\left[\left(\hat{\mathbf{Y}} - \mathbb{E}[\hat{\mathbf{Y}}]\right)\left(\hat{\mathbf{Y}} - \mathbb{E}[\hat{\mathbf{Y}}]\right)^{\mathbf{T}}\right] \tag{60}$$

where the expectation $\mathbb{E}[\quad]$ (taken along the columns of $\hat{\mathbf{Y}}$) is subtracted from each column of the matrix $\hat{\mathbf{Y}}$. Note that the covariance matrix obtained via equation 60 will differ from that of equation 16, which was used for its mathematical convenience.

Under the assumption of operator uncertainty the columns of $\mathbf{Y}$ are independent and as such their covariance is zero. Since relatively few excitations will be applied in practice, these zero elements of $\mathbf{\Sigma_Y}$ will have some finite value. These entries may be discarded and set to zero if the user is confident that no external sources of correlation are present, otherwise they must be retained.

Together, equations 54, 55, 57 and 60 provide an efficient implementation of the proposed propagation framework, for both primal and dual formulations, accounting for both the complex and correlated nature of the underlying uncertainty.

6. Numerical Case Study

In this section we will provide a numerical validation of the proposed propagation framework. Shown in figure 2 is a diagrammatic representation of the study considered. Two free-free beams (source and receiver) are coupled end-to-end such that they form a third (coupled) beam.

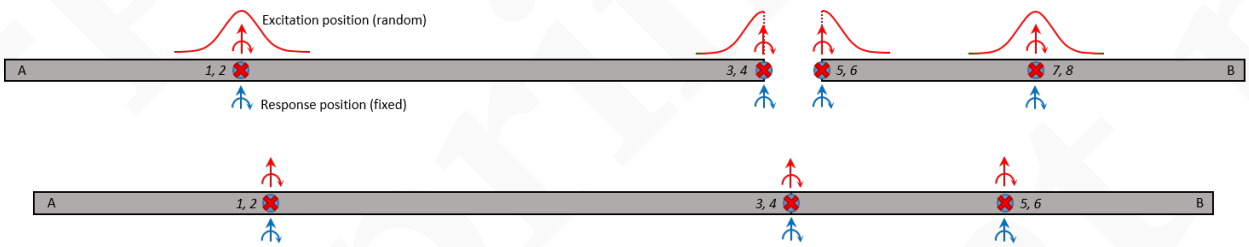

Figure 2: Diagrammatic representation of numerical study. Two free-free beams, A and B, are coupled end-to-end. Measurement and operator uncertainty are modelled using additive noise and randomly distributed excitation positions, respectively. *Uncoupled* DoFs are labelled as follows; internal A translation (1), internal A rotation (2), boundary A translation (3), boundary A rotation (4), boundary B translation (5), boundary B rotation (6), internal B translation (7), and internal B rotation (8). *Coupled* DoFs are labelled as follows; internal A translation (1), internal A rotation (2), boundary translation (3), boundary rotation (4), internal B translation (5), internal B rotation (6).

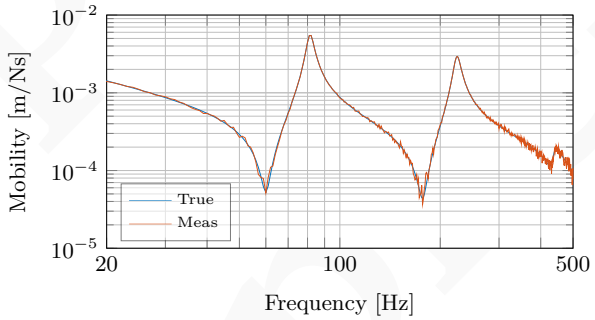

(a) Example FRF 'measurement'. Measurement uncertainty - 20dB SNR.

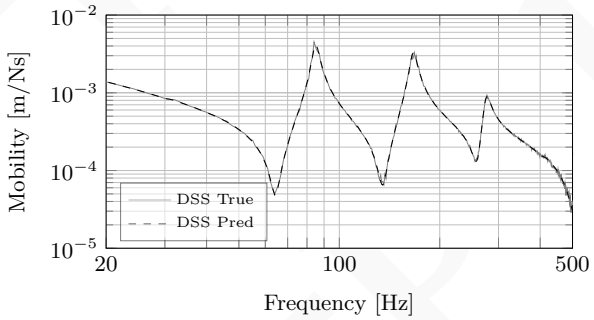

(b) DS prediction based on 'measured' FRFs. Measurement uncertainty - 20dB SNR.

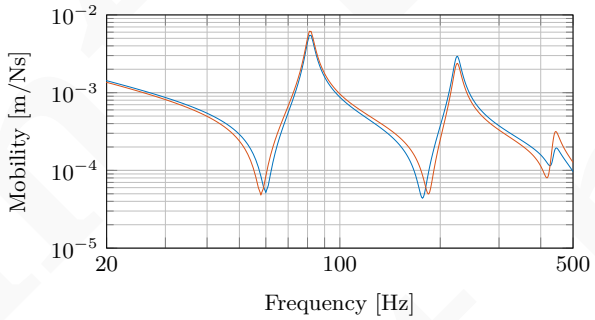

(c) Example FRF 'measurement'. Operator uncertainty - $\sigma^2 = 0.02$.

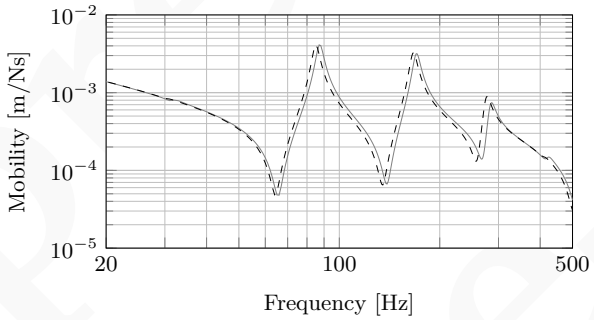

(d) DS prediction based on 'measured' FRFs. Operator uncertainty - $\sigma^2 = 0.02$.

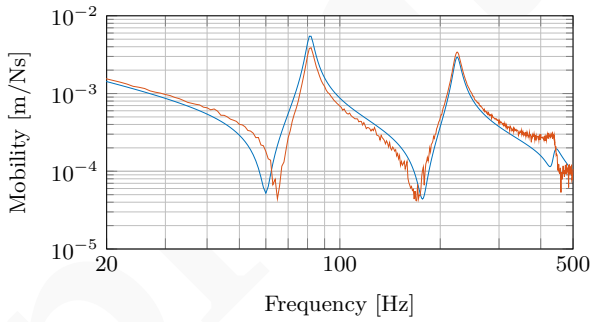

(e) Example FRF 'measurement'. Combined measurement and operator uncertainty - 20dB SNR and $\sigma^2 = 0.02$.

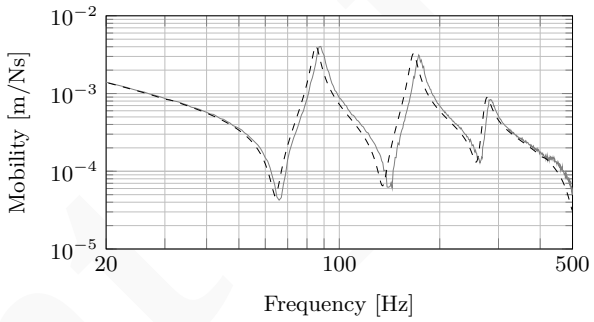

(f) DS prediction based on 'measured' FRFs. Combined measurement and operator uncertainty - 20dB SNR and $\sigma^2 = 0.02$.

Figure 3: Illustrative examples of measurement and operator uncertainty on the point FRF of the source substructure. A single 'measurement' is shown for clarity. Legend description: True (in blue) - the true FRF of uncoupled sub-structure (Y_{S11}), Meas (in orange) - example 'measurement' of uncoupled FRF, DS True (in grey) - the true FRF of the sub-structured assembly (Y_{C11}), DS Pred (in dashed black) - predicted FRF of the sub-structured assembly based on averaged 'measured' FRFs.

The aim of this study is to estimate the uncertainty in the FRFs of the coupled beam, based on the uncertainty of the 'measured' sub-structure FRFs. An analytical beam model was chosen as (1) it represents a simple system that exhibits the physical phenomena expected from operator uncertainty and (2) closed form solutions are available which aid in efficient Monte-Carlo simulations. The measured FRFs are simulated in such a way as to include the effect of both measurement and operator uncertainty. The uncoupled source and receiver sub-structures each have 4 DoFs: 2 internal, and 2 boundary, as illustrated in figure 2. Their free boundary FRFs matrices are given by $\mathbf{Y_S} \in \mathbb{C}^{4\times4}$ and $\mathbf{Y_R} \in \mathbb{C}^{4\times4}$, respectively. Consequently, the coupled assembly FRF is given by $\mathbf{Y_C} \in \mathbb{C}^{6\times6}$. The labelling of coupled

and uncoupled DoFs is provided in the caption of figure 2.

In what follows we will consider 3 scenarios, sub-structuring in: the presence of measurement uncertainty only, the presence of operator uncertainty only, and in the presence of both measurement and operator uncertainty. Here measurement uncertainty will be modelled as an additive noise using a time domain noise model with a random Gaussian distributed amplitude. Operator uncertainty will be modelled by randomly distributing the force and moment excitation positions (see figure 2) and performing repeated 'measurements'.

Shown in figure 3a and 3c are illustrative examples of, respectively, measurement and operator uncertainty on a point FRF of the uncoupled source substructure. Shown in figure 3e is an example of their combined effect. In each figure the true point FRF is shown in blue and a *single* 'measured' FRF is shown in orange. Shown in figures 3b, 3d and 3f are, in grey, the sub-structured point FRF predictions based on a *set* of measured FRFs, and in black the true coupled FRFs.

Notice that the sub-structured prediction for the coupled FRF in the presence of measurement uncertainty only is in good agreement with the true FRF. This is because the measurement uncertainty has a zero mean value and, as such, the expected uncoupled FRFs provide a good estimation of the true uncoupled FRFs. In the presence of operator uncertainty, however, some noticeable shifts are observed. Whilst it was shown in [7] that for a normally distributed excitation position (with low variance) operator uncertainty does not introduce any bias, we note that the boundary DoFs were measured using a half Gaussian distribution (see figure 2). As a result a bias is introduced, the effects of which are seen in the coupled FRFs of figure 3d and 3f.

In each scenario considered the proposed framework (labelled as LEP for 'Law of Error Propagation' in figure legends) is compared against a Monte-Carlo (MC) simulation, which will be regarded as the baseline truth, since it implicitly includes the effect of any correlation and non-linearity present in the uncoupled FRFs and propagation function (i.e equation 13), respectively. The MC simulation involves randomly selecting a subset of measured source and receiver FRF matrices, from the set of all possible matrices, and repeatedly performing the primal (or dual) DS procedure. The statistics of the resulting FRF matrices are then analysed and compared against those obtained through the proposed framework. In the following MC simulations 1000 source and receiver FRF matrices were chosen at random. To highlight the importance of inter-FRF correlation, in each scenario uncertainty will be propagated with and without the influence of inter-FRF correlation. In the latter, only the diagonal elements of $\mathbf{\Sigma_Y}$ are considered. This assumption is in agreement with many previous works (as discussed in section 1), including the DS uncertainty framework presented in [5].

6.1. Measurement Uncertainty

We will begin by considering the propagation of measurement uncertainty only. In the absence of a more realistic model, measurement uncertainty is introduced here via a time domain random noise model with a Gaussian amplitude distribution,

$$p(x) = \frac{1}{\sigma\sqrt{2\pi}} e^{\frac{-(x-\mu)^2}{2\sigma^2}} \tag{61}$$

with zero mean ($\mu = 0$) and variance $\sigma^2 = (5 \times 10^{-7})^2$. For each FRF entry, Y_{ij}, an independent time domain noise vector, $\epsilon_{ij}(t)$, is generated, Fourier transformed and scaled such that the 'measured' FRFs have a signal-to-noise ratio (SNR) of L dB. A suitable scaling is achieved using an energy normalisation formulated as,

$$\epsilon_{ij}(\omega) = 10^{-L/10} \sum_{\omega} Y_{ij}(\omega)^2 \frac{\mathcal{F}\{\epsilon_{ij}(t)\}}{\sum_{\omega} \mathcal{F}\{\epsilon_{ij}(t)\}^2} \tag{62}$$

where, $10^{-L/10}$ is a linear measure of the SNR, $\sum_{\omega} Y_{ij}^2$ is the total energy in the noise free signal, and $\sum_{\omega} \mathcal{F}\{\epsilon(t)\}^2$ is the total energy in the noise signal, where $\mathcal{F}\{\}$ represents the Fourier transform operator. Each $\epsilon_{ij}(\omega)$ is assembled to construct the noise matrix, ϵ. The measured FRF matrix, $\mathbf{Y^{meas}}$, is then given by,

$$\mathbf{Y^{meas}} = \mathbf{Y} + \epsilon. \tag{63}$$

The above is equivalent to adding a frequency independent noise floor to each FRF, which is a reasonable representation of measurement noise.

For each sub-structure 10 measured FRF matrices are simulated, from which the expectations, $\mathbb{E}[\mathbf{Y}_{\mathbf{S}}^{\mathbf{meas}}] \in \mathbb{C}^{4\times4}$ and $\mathbb{E}[\mathbf{Y}_{\mathbf{R}}^{\mathbf{meas}}] \in \mathbb{C}^{4\times4}$, are determined, alongside the bivariate covariance matrices $\mathbf{\Sigma}_{\mathbf{Y_S}} \in \mathbb{R}^{32\times32}$ and $\mathbf{\Sigma}_{\mathbf{Y_R}} \in \mathbb{R}^{32\times32}$. Substituting the expected FRFs into the Jacobian, and using equation 19, one can readily estimate the bivariate uncertainty between any two elements of the coupled FRF matrix, $\mathbf{\Sigma}_{\mathbf{Y_{Cij}},\mathbf{Y_{Clm}}}$.

Shown in figure 4 are the estimated uncertainties in the coupled point FRF Y_{C11} in the presence of measurement uncertainty only. In figure 4a are the relative variance estimates of the real component with (orange) and without (blue) inter-FRF correlation. Also shown is the MC simulation (dashed yellow). Similarly, figure 4b and 4c show the relative variance of and covariance between, the imaginary and real components, respectively. Note that here we define the relative covariance as,

$$\mathrm{RelCov}[A, B] = \frac{\sigma_{AB}}{\mathbb{E}[A]\mathbb{E}[B]}. \tag{64}$$

The agreement observed in figures 4b and 4c suggest that the proposed framework provides an accurate estimate of the real and imaginary variance, whether or not inter-FRF correlations are considered. This is to be expected since the measurement uncertainty considered is uncorrelated at the sub-structure level. However, the neglect of inter-FRF correlation does worsen the estimation of the relative covariance between real and imaginary components, as shown in figure 4c.

Shown in figure 4d is the (predicted) coupled FRF magnitude (yellow) with the 95% confidence intervals (for an assumed log normal distribution) associated with the estimated uncertainty with and without the influence of inter-FRF correlations. The two confidence bounds are almost perfectly overlayed, suggesting that the disagreement in the relative covariance (figure 4c) has a minimal effect when propagating the estimated uncertainty further through the magnitude function as per equation 7.

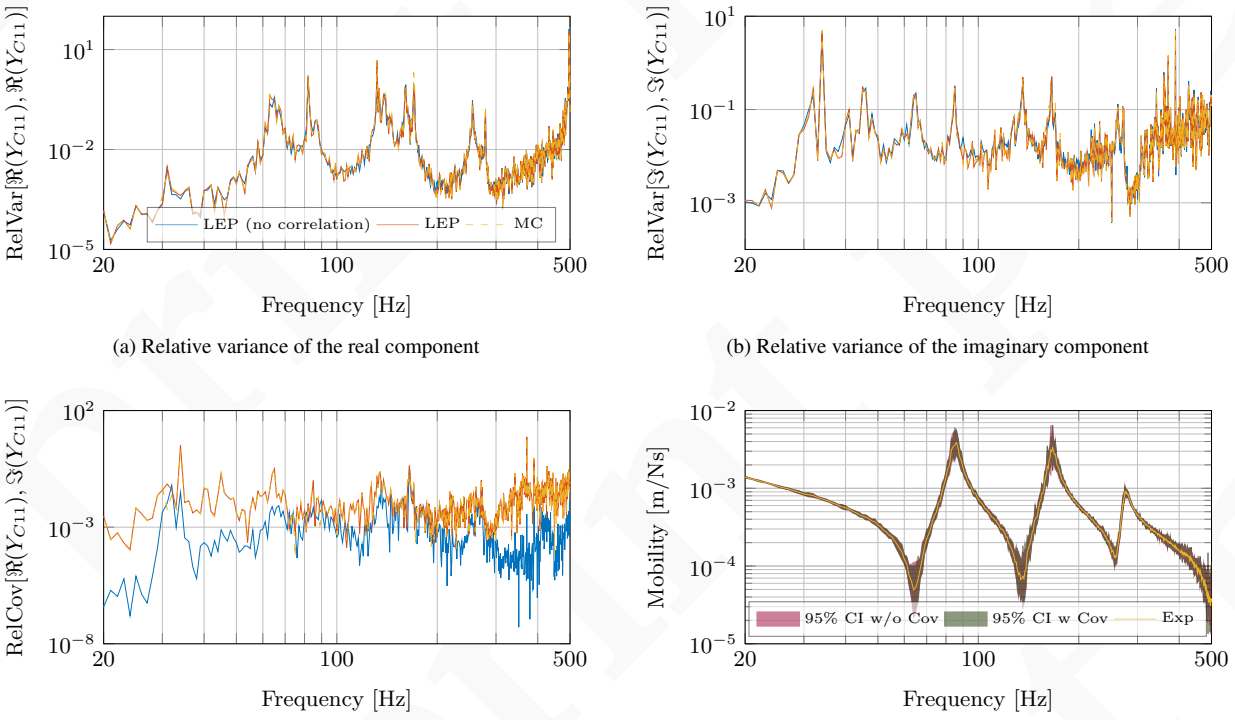

(a) Relative variance of the real component

(b) Relative variance of the imaginary component

(c) Relative covariance between the real and imagainary components

(d) Coupled FRF magnitude and 95% confidence interval (with and without inter-FRF correlations)

Figure 4: Bivariate uncertainty estimates in the sub-structured FRF Y_{C11} due to the presence of measurement uncertainty only with an SNR of 20 dB. Legend description: LEP (no correlation) - framework based estimate neglecting the influence of correlation between sub-structure FRFs, LEP - framework based estimate including all correlations, MC - estimate based on Monte-Carlo simulation. The LEP (no correlation) estimate is obtained by taking only the diagonal elements of $\mathbf{\Sigma}_{\mathbf{Y}}$.

The use of a log normal distribution for the FRF magnitude was chosen simply as a mean of presenting the results of figures 4a-4c in a more intuitive way. For a small Gaussian input uncertainty the bivariate output uncertainty of a sub-structured FRF (as predicted by the proposed framework) remains Gaussian, since we have considered a linear propagation of uncertainty. Consequently, the range of possible values for the real and imaginary components extend from $-\infty$ to $+\infty$. The magnitude of the FRF however, is strictly positive, and so a Gaussian distribution is no longer appropriate. It is for this reason that we have chosen to present the confidence bound using a log normal distribution (which is strictly positive). The true underlying distribution is more complex however, and is treated analytically in [32]. Nevertheless, for the purpose of presentation the log normal distribution is considered sufficient here.

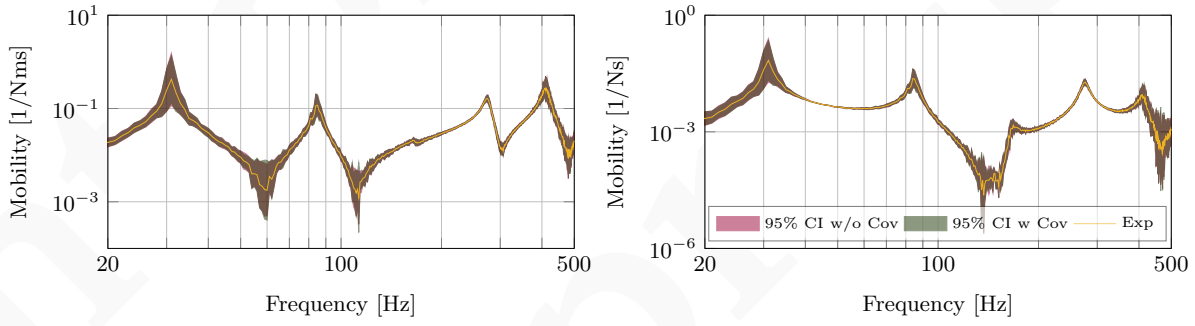

(a) Rotational driving point FRF Y_{C22}

(b) Translational-rotationalal transfer FRF Y_{C23}

Figure 5: Coupled FRF magnitude and 95% confidence interval (with and without inter-FRF correlations) for the sub-structured FRFs Y_{C22} (a) and Y_{C23} (b) due to the presence of measurement uncertainty only with an SNR of 20 dB.

For completeness figure 5 shows the confidence intervals obtained for two other sub-structured FRFs, the driving point rotational FRF Y_{C22} and the transfer translations-rotational FRF Y_{C23}. Again, given the uncorrelated input uncertainty, the two confidence bounds are in good agreement.

6.2. Operator Uncertainty

Having considered measurement uncertainty above, we will now consider the propagation of operator uncertainty. To model the effect of operator uncertainty (i.e. the uncertainty in excitation position due to human error) the excitation position for each DoF is varied randomly according to Gaussian distribution. In the case of the interface DoFs a single sided Gaussian distribution is used, as illustrated in figure 2. The excitation distributions are centred about the intended position with the degree of operator uncertainty set by the standard deviation $\sigma = 0.02$.[4] The measured FRFs thus take the form,

$$\mathbf{Y}^{\mathbf{meas}} = \mathbf{Y}(a_0 + \mathbf{a}) \tag{65}$$

where $\mathbf{Y}()$ represents an FRF function whose argument $a_0 + \mathbf{a}$ denotes the excitation position, such that $\mathbf{a} \sim \mathcal{N}(0, \sigma^2)$.

For each sub-structure 10 'measurements' are performed at each DoF, from which the expectations, $\mathbb{E}[\mathbf{Y}_{\mathbf{S}}^{\mathbf{meas}}] \in \mathbb{C}^{4\times4}$ and $\mathbb{E}[\mathbf{Y}_{\mathbf{R}}^{\mathbf{meas}}] \in \mathbb{C}^{4\times4}$, are determined, alongside the bivariate covariance matrices $\mathbf{\Sigma}_{\mathbf{Y_S}} \in \mathbb{R}^{32\times32}$ and $\mathbf{\Sigma}_{\mathbf{Y_R}} \in \mathbb{R}^{32\times32}$. To estimate the bivariate covariance matrices we note that only the elements of $\mathbf{Y}$ that share an excitation position are correlated. As such, $\mathbf{\Sigma}_{\mathbf{Y_S}} \in \mathbb{R}^{32\times32}$ and $\mathbf{\Sigma}_{\mathbf{Y_R}} \in \mathbb{R}^{32\times32}$ are constructed by taking, separately, the columns of their respective FRF matrices, computing their covariances, and block diagonalising the resulting matrices appropriately [7].

Shown in figure 6 are the estimated uncertainties in the coupled point FRF Y_{C11} in the presence of operator uncertainty only. In figure 6a are the relative variance estimates of the real component with (orange) and without (blue) inter-FRF correlation. Also shown is the MC simulation (dashed yellow). Similarly, figure 6b and 6c show

[4] It should be noted that in a practical scenario the severity of operator uncertainty will vary greatly depending on multiple factors, including: experience of the experimenter, access to the measurement positions, the local dynamics of the structure, etc. We have chosen $\sigma = 0.02$ as a conservative level of uncertainty in that it corresponds, roughly, to an excitation within ±4cm of the intended position 95% of the time.

the relative variance of, and the covariance between, the imaginary and real components, respectively. In contrast to the measurement uncertainty considered above, there are clear discrepancies between the uncertainty estimates with and without inter-FRF correlation, the former remaining in good agreement with MC simulations. This disagreement is expected, since the notion of operator uncertainty introduces a correlation between measured FRFs, which is not propagated when the off-diagonal terms of $\mathbf{\Sigma_Y}$ are neglected. Agreement between the proposed framework (with inter-FRF correlation) and MC simulations suggest that a correct propagation of uncertainty has been achieved. However, some small discrepancies are still observed. These are a result of the linear approximation employed in the law of error propagation. For a greater level of uncertainty this discrepancy might be expected to increase.

It is interesting to note that the discrepancies due to the neglect of inter-FRF correlation do not appear to coincide in particular with regions of large relative variance, although they do tend to lead to an over-estimation of uncertainty. This over-estimation is more clearly observed in figure 6d where the estimated confidence bounds on the coupled FRF magnitude are shown. It is clear, in this case at least, that the neglect of inter-FRF correlation in the propagation of uncertainty leads to much a wider confidence bound on the resultant FRF. In practical terms this is interesting as knowledge of the inter-FRF correlation in the uncoupled sub-structures may be obtained at little additional effort over and above standard variance estimates, yet its introduction appears to lead to increased confidence in the coupled FRFs.

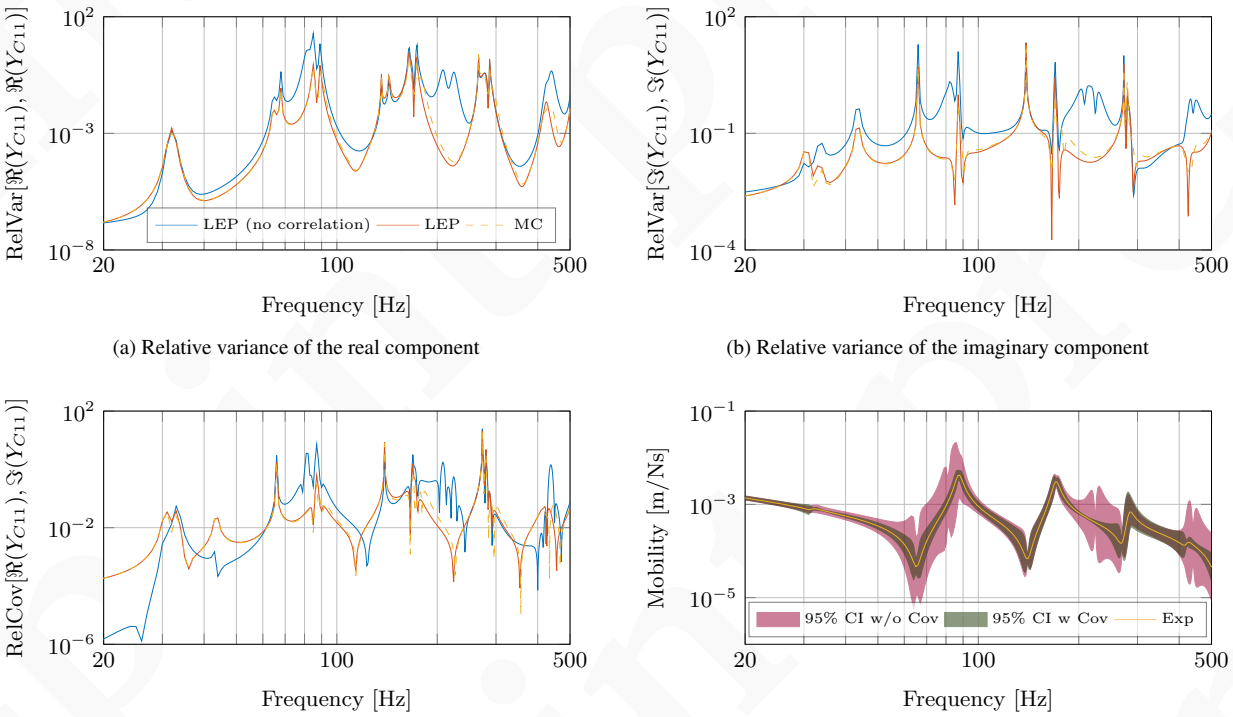

(a) Relative variance of the real component

(b) Relative variance of the imaginary component

(c) Relative covariance between the real and imagainary components

(d) Coupled FRF magnitude and 95% confidence interval (with and without inter-FRF correlations)

Figure 6: Bivariate uncertainty estimates in the sub-structured FRF Y_{C11} due to the presence of operator uncertainty only with a excitation variance of $\sigma = 0.02$. Legend description: LEP (no correlation) - framework based estimate neglecting the influence of correlation between sub-structure FRFs, LEP - framework based estimate including all correlations, MC - estimate based on Monte-Carlo simulation. The LEP (no correlation) estimate is obtained by taking only the diagonal elements of $\mathbf{\Sigma_Y}$.

6.3. Combined Uncertainty

Finally, in this section we will consider the propagation of both measurement and operator uncertainty. Each uncertainty is modelled as described above. The measured FRF matrix is consequently given by,

$$\mathbf{Y}^{\mathbf{meas}} = \mathbf{Y}(a_0 + \mathbf{a}) + \epsilon. \tag{66}$$

Shown in figure 7 are the estimated uncertainties in the coupled point FRF Y_{C11} in the presence of both measurement and operator uncertainty. In figure 7a are the relative variance estimates of the real component with (orange) and without (blue) inter-FRF correlation. Also shown is the MC simulation (dashed yellow). Similarly, figure 7b and 7c show the relative variance of, and covariance between, the imaginary and real components, respectively.

The results presented through figure 7 are expected on the basis of figures 4 and 6. It can be seen that in regions dominated by measurement uncertainty, the proposed framework provides an accurate estimation of uncertainty regardless of whether inter-FRF correlations are considered. This accurate estimation is permeated by regions dominated by operator uncertainty. In these regions inter-FRF correlations are essential for an accurate estimation of uncertainty.

As in figure 6d, in the presence of both measurement and operator uncertainty figure 7d demonstrates that knowledge of the inter-FRF correlations present can lead to an increased confidence in the predicted FRFs. A similar result was also obtained in [7] based on *experimentally* measured FRFs and the propagation of uncertainty through a matrix inversion. These results support the use of more general treatments of uncertainty, such that inter-FRF correlations are accounted for.

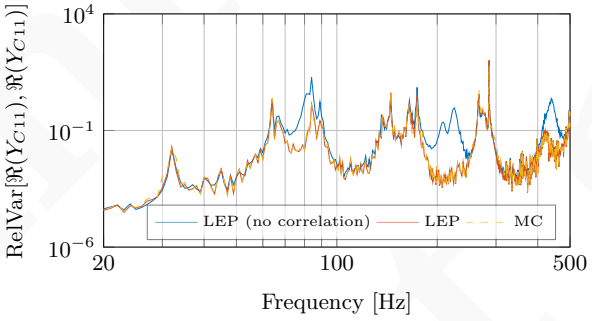

(a) Relative variance of the real component

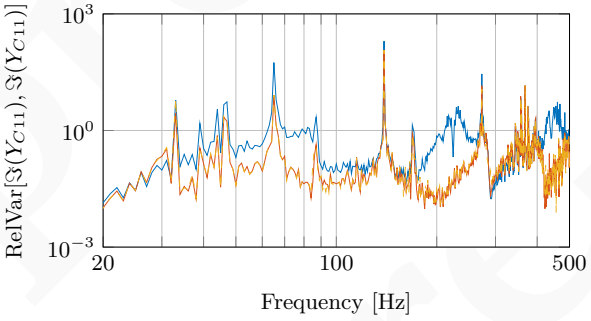

(b) Relative variance of the imaginary component

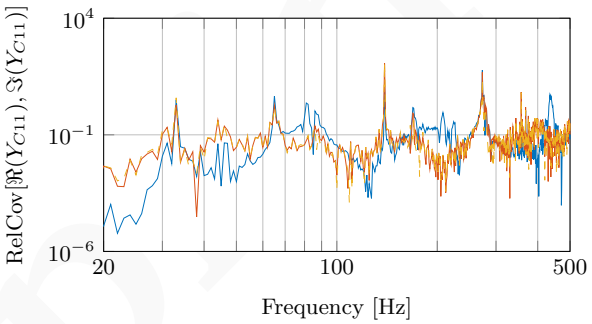

(c) Relative covariance between the real and imagainary components

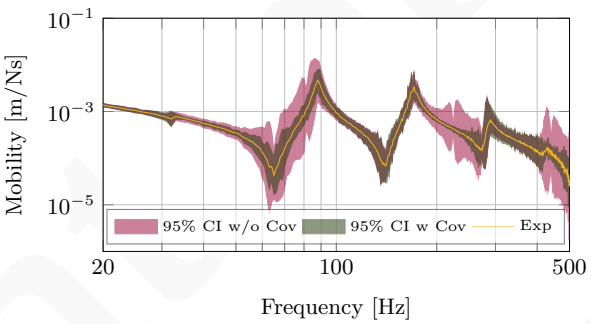

(d) Coupled FRF magnitude and 95% confidence interval (with and without inter-FRF correlations)

Figure 7: Bivariate uncertainty estimates in the sub-structured FRF Y_{C11} due to the presence of both measurement (SNR = 20dB) and operator ($\sigma^2 = 0.02$) uncertainty. Legend description: LEP (no correlation) - framework based estimate neglecting the influence of correlation between sub-structure FRFs, LEP - framework based estimate including all correlations, MC - estimate based on Monte-Carlo simulation. The LEP (no correlation) estimate is obtained by taking only the diagonal elements of $\mathbf{\Sigma_Y}$.

The results presented in this section, although of a numerical simulation, are representative of real physical structures and provide a validation of the proposed framework. It is important to reiterate, however, that the linear covariance propagation considered here is valid only in the presence of small uncertainty, given that the propagation function is non-linear. For larger levels of uncertainty one may establish a second order propagation framework as was done in [5], or utilise the MC simulation approach. Nevertheless, the proposed framework may prove useful, for example, in investigating the contribution of an uncoupled FRF uncertainty to that of the coupled assembly. As an example, in

section 6.4 we will consider a benefit analysis/rank ordering of uncertainty for the numerical study considered.

6.4. Benefit Analysis and Rank Ordering

In an industrial setting it may be required that an FRF prediction satisfies some specified level of confidence as structures are often designed to conform to strict limits. If the uncertainty of a particular FRF exceeds a given limit, we may wish to improve our confidence in the predicted FRF. Naively, we might repeat all measurements in the hope that better results are obtained the second time round. This would be inefficient, both practically and financially. Alternatively, using the uncertainty propagation we may perform a rank ordering (of-sorts) to identify the uncoupled FRFs that contribute most significantly to the uncertainty of the coupled FRF in question. Having identified the dominant source(s) of uncertainty, the benefit, in terms of potential uncertainty reduction given the financial/practical cost, of repeating these FRF measurements may be deliberated.

As an example, in this section we will attempt to identify the dominant source of uncertainty for the boundary-internal transfer FRF Y_{C35}, which relates the translational force at the source-receiver boundary, to the translational response at the internal receiver DoF (see the caption of figure 2 for DoF labelling). We will consider the case where both measurement and operator uncertainty are present. To simulate a more realistic scenario, each FRF measurement (i.e. column of the FRF matrix) is assigned a different level of operator uncertainty, varying between $\sigma = 0.001$ and $\sigma = 0.02$.

To identify the dominant source of uncertainty the covariance matrices associated with each column of the measured FRF matrices are propagated separately. This is achieved by setting all other covariance terms in $\mathbf{\Sigma_Y}$ to zero and performing the propagation in the standard way, as per section 4. The source and receiver sub-structures are each characterised by four DoFs, two internal and two boundary. As such, there are a total of 8 'measurements' whose uncertainty we wish to propagate.

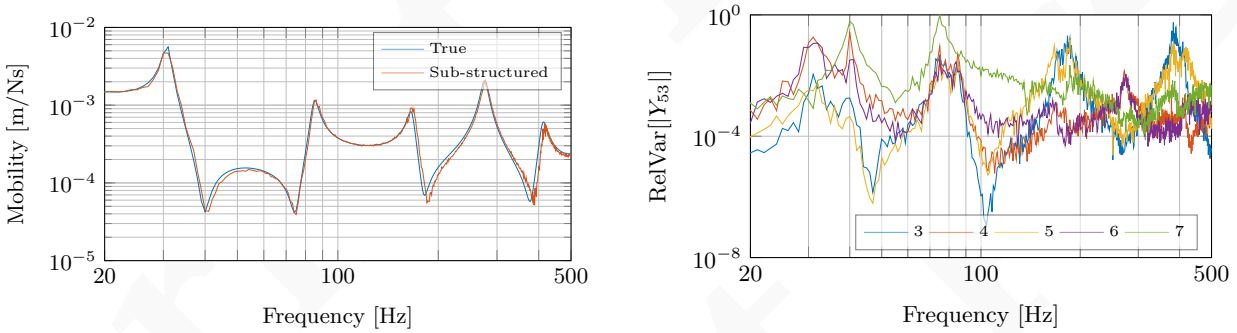

(a) Transfer function magnitude $|Y_{53}|$

(b) Relative variance contributions due to uncertain excitations.

Figure 8: Rank ordering of the contributions to $\sigma_{|Y_{C53}|}$ due to uncoupled sub-structure FRF measurements. In (a) are the true and sub-structured FRF prediction for $|Y_{C53}|$. In (b) are the relative variance contributions. The legend entries correspond to the DoF of the measurement, i.e. '3' is the relative variance contribution due to the uncoupled FRFs measured when exciting DoF 3. DoFs 1, 2 and 8 contributed a negligible amount so have not been plotted.

Shown in figure 8 are the results of the uncertainty propagation. In figure 8a is the true FRF $|Y_{C53}|$ (blue), and its sub-structured prediction (orange). In figure 8b are the contributions to the uncertainty (relative variance) of $|Y_{C53}|$ due to each of the uncoupled FRF 'measurements'. Each plot corresponds to the uncertainty contribution arising from a column of the uncoupled FRF matrix $\mathbf{Y}$. From figure 8b we are able to draw the following conclusions. To improve confidence about the first (and fourth) resonance we should repeat the measurements at DoFs 4 and 6 (i.e. rotational boundary excitations). To improve confidence about the third (and fifth) resonance we should repeat the measurements at DoFs 3 and 5 (i.e. translational boundary excitations). To improve confidence about the second resonance we should repeat the translational excitation at the internal receiver DoF 7. In fact, figure 8b suggests that repeating the excitation of DoF 7 would provide the single greatest improvement in the overall uncertainty, particularly in the range of 35-150 Hz. The contributions due to DoFs 1, 2 and 8 were negligible and not shown. This is in agreement with the notion that the uncertainties related to internal DoFs tend not to propagate so far as boundary DoFs (see section 4.3).

Although of a simple numerical model, the above results illustrate the application of the proposed framework in the context of a benefit analysis which may be of use in practical situations where we wish to improve our confidence in a given FRF prediction.

7. Conclusions

This paper has been concerned with the propagation of correlated FRF uncertainty through dynamic sub-structuring procedures. A covariance based framework is derived for propagating both complex and correlated uncertainty through primal and dual sub-structuring procedures. By symmetry of the underlying equations, the proposed framework is valid also in the case of sub-structure decoupling.

The framework was largely motived by the notion of operator uncertainty (due to inconsistent force excitations in FRF measurements) and the inter-FRF correlation that it introduces. In this regard, the proposed framework provides a more general treatment of uncertainty in DS.

Through an algebraic example the conclusions drawn by Voormeeren et al. [5], regarding the propagation of *uncorrelated* uncertainty, were substantiated. Using the proposed framework further conclusions were drawn regarding the propagation and influence of *correlated* uncertainty. Specifically, it was shown that, if neglected, the presence of inter-FRF correlation in *any* uncoupled sub-structure can lead to an incorrect estimation of the uncertainty in *all* coupled FRFs. This result was further demonstrated as part of a numerical study, and justifies use of the proposed framework.

To aid in the efficient implementation of the proposed framework, simplified constructions of both primal and dual Jacobian matrices were demonstrated. Application of the framework in the context of a benefit analysis/rank ordering was further illustrated, where dominant sources of uncertainty were identified as part of a numerical study.

The proposed framework has been validated against Monte-Carlo simulations in the presence of measurement uncertainty (uncorrelated), operator uncertainty (correlated), and a combination thereof. The influence of inter-FRF correlation was further investigated by neglecting the off-diagonal elements of the uncoupled FRF covariance matrix. Results suggest that the added complexity involved in propagating *correlated* uncertainty is justified given the improved confidence in coupled FRFs predictions, which would otherwise be subject to large over-conservative estimates of uncertainty.

As a final remark, the uncertainty framework proposed herein, together with that of [10], provide the necessary tools to estimate response uncertainty in complex built-up structures whilst under operational conditions, for example, in the construction of a Virtual Acoustic Prototype, or in a component-based TPA.

Acknowledgements

This work was funded through the EPSRC Research Grant EP/P005489/1 Design by Science.

Appendix A. Law of Error Propagation

In this section we will derive, for completeness, the law of error propagation. We begin by considering the variables x_i and x_j, generally, as the outputs of some multi-variable function,

$$x_i = G_i(a_1, a_2, a_3, \cdots) = G_i(\mathbf{a}) \tag{A.1}$$

$$x_j = G_j(a_1, a_2, a_3, \cdots) = G_j(\mathbf{a}). \tag{A.2}$$

Suppose that we repeatedly measure values of the input variables $\mathbf{a}$, denoting the nth measurement by the subscript n. It is clear that a small change in the value of $\mathbf{a}$ will lead to a small change in the value of the output variables x_i and x_j. Assuming that these changes remain small, they may be approximated to first order by a Taylor series expansion.

$$\Delta x_{i_n} = \frac{\partial G_i(\mathbf{a})}{\partial a_1}\Delta a_{1_n} + \frac{\partial G_i(\mathbf{a})}{\partial a_2}\Delta a_{2_n} + \cdots + \frac{\partial G_i(\mathbf{a})}{\partial a_l}\Delta a_{l_n} \tag{A.3}$$

$$\Delta x_{j_n} = \frac{\partial G_j(\mathbf{a})}{\partial a_1}\Delta a_{1_n} + \frac{\partial G_j(\mathbf{a})}{\partial a_2}\Delta a_{2_n} + \cdots + \frac{\partial G_j(\mathbf{a})}{\partial a_m}\Delta a_{m_n} \tag{A.4}$$

We are interested in determining the covariance between the output variables x_i and x_j. As such, we begin by multiplying together equation A.3 and A.4,

$$\Delta x_{i_n} \Delta x_{j_n} = \left(\sum_l \frac{\partial G_i(\mathbf{a})}{\partial a_l} \Delta a_{l_n} \right) \left(\sum_m \frac{\partial G_j(\mathbf{a})}{\partial a_m} \Delta a_{m_n} \right). \tag{A.5}$$

Expanding the brackets,

$$\Delta x_{i_n} \Delta x_{j_n} = \frac{\partial G_i(\mathbf{a})}{\partial a_1} \Delta a_{1_n} \left(\sum_m \frac{\partial G_j(\mathbf{a})}{\partial a_m} \Delta a_{m_n} \right) + \frac{\partial G_i(\mathbf{a})}{\partial a_2} \Delta a_{2_n} \left(\sum_m \frac{\partial G_j(\mathbf{a})}{\partial a_m} \Delta a_{m_n} \right) + \cdots + \frac{\partial G_i(\mathbf{a})}{\partial a_l} \Delta a_{l_n} \left(\sum_m \frac{\partial G_j(\mathbf{a})}{\partial a_m} \Delta a_{m_n} \right) \tag{A.6}$$

and summing over N measurements whilst dividing both sides by $\frac{1}{N-1}$, and noting the covariance relation $\sigma_{a_l a_m} = \frac{1}{N-1} \sum_n^N \Delta a_{l_n} \Delta a_{m_n}$, we arrive at,

$$\sigma_{x_i x_j} = \sum_l^M \frac{\partial G_i(\mathbf{a})}{\partial a_l} \frac{\partial G_j(\mathbf{a})}{\partial a_l} \sigma_{a_l a_l} + \sum_{m \neq l} \frac{\partial G_i(\mathbf{a})}{\partial a_l} \frac{\partial G_j(\mathbf{a})}{\partial a_m} \sigma_{a_l a_m}. \tag{A.7}$$

The above may be expressed more conveniently in matrix form as,

$$\sigma_{x_i x_j} = \mathbf{J_i} \mathbf{\Sigma_a} \mathbf{J_j^T} \tag{A.8}$$

where,

$$\mathbf{J_i} = \begin{bmatrix} \frac{\partial G_i(\mathbf{a})}{\partial a_1} & \frac{\partial G_i(\mathbf{a})}{\partial a_2} & \cdots & \frac{\partial G_i(\mathbf{a})}{\partial a_M} \end{bmatrix} \tag{A.9}$$

$$\mathbf{J_j} = \begin{bmatrix} \frac{\partial G_j(\mathbf{a})}{\partial a_1} & \frac{\partial G_j(\mathbf{a})}{\partial a_2} & \cdots & \frac{\partial G_j(\mathbf{a})}{\partial a_M} \end{bmatrix} \tag{A.10}$$

are the Jacobians of the functions $x_i = G_i(\mathbf{a})$ and $x_j = G_j(\mathbf{a})$, respectively, and $\mathbf{\Sigma_a}$ is the variance-covariance matrix of the input vector $\mathbf{a}$.

$$\mathbf{\Sigma_a} = \begin{bmatrix} \sigma_{a_1 a_1} & \sigma_{a_1 a_2} & \cdots & \sigma_{a_1 a_M} \\ \sigma_{a_2 a_1} & \sigma_{a_2 a_2} & \cdots & \sigma_{a_2 a_M} \\ \vdots & \vdots & \ddots & \vdots \\ \sigma_{a_M a_1} & \sigma_{a_M a_2} & \cdots & \sigma_{a_M a_M} \end{bmatrix} \tag{A.11}$$

Equations A.8-A.11 describe, generally, the law of error propagation.

Appendix B. Bivariate Derivatives of the Primal Jacobian

The complex differential of the primal formulation is given by,

$$d\mathbf{Y_C} = \mathbf{Y_C} \mathbf{L} \mathbf{Y^{-1}} \mathbf{P_{st}} \mathbf{Y^{-1}} \mathbf{L^T} \mathbf{Y_C} dY_{st}. \tag{B.1}$$

Denoting $\mathbf{A} = \mathbf{Y_C} \mathbf{L} \mathbf{Y^{-1}} \mathbf{P_{st}} \mathbf{Y^{-1}} \mathbf{L^T} \mathbf{Y_C}$, and taking the real part of $d\mathbf{Y_C}$,

$$\Re \left(d\mathbf{Y_C} \right) = \Re \left(\mathbf{A} dY_{st} \right). \tag{B.2}$$

Recalling that $\Re([a + ib][c + id]) = ac - bd$, equation B.2 may be rewritten as,

$$\Re \left(d\mathbf{Y_C} \right) = \left[\Re(\mathbf{A}) \Re(dY_{st}) - \Im(\mathbf{A}) \Im(dY_{st}) \right]. \tag{B.3}$$

Similarly, recalling that $\Im([a + ib][c + id]) = ad + bc$, the imaginary part of differential may be rewritten as,

$$\Im \left(d\mathbf{Y_C} \right) = \left[\Re(\mathbf{A}) \Im(dY_{st}) + \Im(\mathbf{A}) \Re(dY_{st}) \right]. \tag{B.4}$$

From equation B.3 and B.4, it is recognised that,

$$\frac{\partial \Re(\mathbf{Y_C})}{\partial \Re(Y_{st})} = \Re\left(\frac{\partial \mathbf{Y_C}}{\partial Y_{st}}\right), \quad \frac{\partial \Re(\mathbf{Y_C})}{\partial \Im(Y_{st})} = \Im\left(-\frac{\partial \mathbf{Y_C}}{\partial Y_{st}}\right), \quad \frac{\partial \Im(\mathbf{Y_C})}{\partial \Re(Y_{st})} = \Im\left(\frac{\partial \mathbf{Y_C}}{\partial Y_{st}}\right), \quad \frac{\partial \Im(\mathbf{Y_C})}{\partial \Im(Y_{st})} = \Re\left(\frac{\partial \mathbf{Y_C}}{\partial Y_{st}}\right). \tag{B.5}$$

The above equations constitute the Cauchy-Riemann relations, and may be summarised by the complex matrix mapping operator (see equation 28),

$$M(\quad) = \begin{bmatrix} \Re(\quad) & -\Im(\quad) \\ \Im(\quad) & \Re(\quad) \end{bmatrix}. \tag{B.6}$$

References

[1] D. de Klerk, D.J. Rixen, and S.N. Voormeeren. General framework for dynamic substructuring: history, review and classification of techniques. *AIAA Journal*, 46(5):1169–1181, may 2008.

[2] B. R. Mace and K. Worden. Uncertainty in structural dynamics, 2005.

[3] R. A. Ibrahim. Structural dynamics with parameter uncertainties. *Applied Mechanics Reviews*, 40(3), 1987.

[4] C. Soize. A comprehensive overview of a non-parametric probabilistic approach of model uncertainties for predictive models in structural dynamics. *Journal of Sound and Vibration*, 288(3):623–652, 2005.

[5] S.N. Voormeeren, D. de Klerk, and D.J. Rixen. Uncertainty quantification in experimental frequency based substructuring. *Mechanical Systems and Signal Processing*, 24(1):106–118, 2010.

[6] S.N. Voormeeren and D.J. Rixen. Substructure decoupling techniques – a review and uncertainty propagation analysis. *27th International Modal Analysis Conference (IMAC XXVII)*, (January 2009), 2009.

[7] J.W.R. Meggitt. On the treatment of uncertainty in experimentally measured frequency response functions. *Metrologia*, 55:806–818, 2018.

[8] D.C. Kammer and D. Krattiger. Propagation of uncertainty in substructured spacecraft using frequency response. *AIAA Journal*, 51(2):353–361, 2013.

[9] D.C. Kammer and S. Nimityongskul. Propagation of uncertainty in test-analysis correlation of substructured spacecraft. *Journal of Sound and Vibration*, 330(6):1211–1224, 2011.

[10] J.W.R. Meggitt, A.S. Elliott, and A.T. Moorhouse. A covariance based framework for the propagation of uncertainty through inverse problems with an application to force identification. *Mechanical Systems and Signal Processing*, 2018.

[11] J.W.R. Meggitt, A.S. Elliott, and A.T. Moorhouse. Virtual assemblies and their use in the prediction of vibro-acoustic responses. In *Proceedings of the Institute of Acoustics*, Warickshire, 2016.

[12] A.T Moorhouse. Virtual acoustic prototypes: Listening to machines that don't exist. In *Acoustics Australia*, volume 33, pages 97–105, 2005.

[13] A.S. Elliott, A.T. Moorhouse, and G. Pavić. Moment excitation and the measurement of moment mobilities. *Journal of sound and vibration*, 331(1):2499–2519, 2012.

[14] A.T. Moorhouse and A.S. Elliott. The "round trip" theory for reconstruction of Green's functions at passive locations. *The Journal of the Acoustical Society of America*, 134(5):3605–3612, nov 2013.

[15] M. van der Seijs, D. D. van den Bosch, D. J. Rixen, and D. De Klerk. An Improved Methodology for the Virtual Point Transformation of Measured Frequency Response Functions in Dynamic Substructuring. In *ECCOMAS Thematic Conference on Computational Methods in Structural Dynamics and Earthquake Engineering*, Kos Island, Greece, 2013.

[16] A. Drozg, G. Čepon, and M. Boltežar. Full-degrees-of-freedom frequency based substructuring. *Mechanical Systems and Signal Processing*, 98:570–579, 2018.

[17] S.W.B Klaassen, M. van der Seijs, and D. de Klerk. System Equivalent Model Mixing. *Mechanical Systems and Signal Processing*, 105:90–112, 2018.

[18] J.S. Bendat and A.G. Piersol. *Engineering Applications of Correlation and Spectral Analysis*. John Wiley & Sons, Inc., 2nd edition, 1993.

[19] Z. Mao and M. Todd. Statistical modeling of frequency response function estimation for uncertainty quantification. *Mechanical Systems and Signal Processing*, 38(2):333–345, 2013.

[20] D. de Klerk. How Bias Errors Affect Experimental Dynamic Substructuring. In *IMAC XVIII*, pages 1101–1112, 2010.

[21] H.S. Kim and T.L. Schmitz. Bivariate uncertainty analysis for impact testing. *Measurement Science and Technology*, 18(11):3565–3571, 2007.

[22] T. Schultz, M. Sheplak, and L.N. Cattafesta. Application of multivariate uncertainty analysis to frequency response function estimates. *Journal of Sound and Vibration*, 305(1-2):116–133, 2007.

[23] J.S. Bendat and A.G. Piersol. *Random Data: Analysis and Measurement Procedures*. 2011.

[24] F. Fahy and J. Walker. *Advance Applications in Acoustics, Noise and Vibration*. Spoon Press, 2004.

[25] N.M. Ridler and M.J. Slater. An approach to the treatment of uncertainty in complex -parameter measurements. *Metrologia*, 39(3):295–302, 2002.

[26] B.D. Hall. On the propagation of uncertainty in complex-valued quantities. *Metrologia*, 41(3):173–177, 2004.

[27] Seppo Mustonen. A measure for total variability in multivariate normal distribution. *Computational Statistics & Data Analysis*, 23(3):321–334, 1997.

[28] W. D'Ambrogio and A. Fregolent. Direct decoupling of substructures using primal and dual formulation. In *Linking Models and Experiments, Conference Proceedings of the Society for Experimental Mechanics Series*, pages 47–76, 2011.

[29] S.N. Voormeeren and D.J. Rixen. A family of substructure decoupling techniques based on a dual assembly approach. *Mechanical Systems and Signal Processing*, 27:379–396, feb 2012.

[30] A. Hjorunges. *Complex-Valued Matrix Derivatives*. Cambridge University Press, 1st edition, 2011.

[31] G. Strang. *Computational Science and Engineering*. Wellesley-Cambridge Press, 1st edition, 2007.
[32] P. Dharmawansa, N. Rajatheva, and C. Tellambura. Envelope and phase distribution of two correlated gaussian variables. *IEEE Transactions on Communications*, 57(4):915–921, 2009.